ADVANCES IN PHYSICS, 1986, VOL 35, NO 4, 375 422

Aharonov–Bohm effect in normal metal
Quantum coherence and transport

By SEAN WASHBURN and RICHARD A WEBB
IBM T J Watson Research Center, P O Box 218,
Yorktown Heights, New York 10598, U S A

[Received 13 October 1986]

Abstract

We review some of the recent surprising theoretical and experimental results obtained on the transport properties of small disordered metal samples Even in the presence of disorder, the quantum mechanical interference of electron wavefunctions can still be observed The Aharonov Bohm effect is a particularly clear demonstration of this In doubly connected structures (such as loops of wire) threaded by a magnetic flux, the electrical conductance oscillates because of the Aharonov–Bohm effect In fact, because the electron trajectories are diffusive (i e random walks), even a lone wire (a singly connected structure) will exhibit a random pattern of conductance fluctuations as a function of the magnetic field because of the same interference effects All that is required for the observation of these interferences is that the electrons retain 'phase memory' during the period of transit through the sample The length over which memory is maintained (the phase coherence length) can be much larger than the random walk step length (the mean free path) We focus mainly on effects observed in the limit where the phase coherence length of the electrons is comparable to or larger than the sample size We explain how the interferences are averaged as the system size grows larger than the phase coherence length We also remark on surprising aspects of the fluctuations such as those resulting from the non-local character of the wavefunction, some of the results are forbidden classically

Contents

1 Introduction

The standard approach to calculating the electrical resistance of systems that contain large numbers of particles is to assume some distribution of scatterers, average over all possible distributions of these scatterers, and take the limit of the scattering rate as the size of the system approaches infinity This is known as the thermodynamic limit The ohmic resistance of a wire is an example of an average property that can be computed in this fashion The wire in question is assumed to be of homogeneous metal in which the electrons move ballistically for a distance l (the mean free path), scatter, move ballistically again, and so on The velocity correlations (the current through the wire is proportional to the average velocity of the electrons), when averaged over many collisions, can predict the conductance of any piece of wire which has the same average density of scattering sites If we were to consider only some very small volume of the wire, it is clear that, not only would the resistance of this section be different from the average of the whole system, but the quantum-mechanical characteristics of both the electrons and scattering sites would have to be known in order to calculate the resistance This is the difference between physics at the microscopic level and macroscopic level The usual Boltzmann approach to calculating transport coefficients (such as conductivity) by averaging the velocity [1] breaks down at the microscopic level The question is then How large must the system be so that the microscopic details of the transport can be approximated by some average distribution? The surprising answer is that the system must be much larger than the distance the electron travels before suffering phase randomizing collisions Elastic scattering does not cause the electrons to lose phase memory, only inelastic processes are important for determining this size At low temperatures this distance can be very large many millimetres in some cases

The miniaturization of electronics has now reached the stage where devices can be fabricated at lengths of less than one micron In such devices, the electrons can traverse the sample coherently -the quantum-mechanical wavefunction maintains its phase coherence all the way across the sample This access to 'coherent transport' granted by the advances in lithography has opened a very rich field of theoretical and experimental physics Experimentalists can now build devices that permit the study of the quantum-mechanical properties of a large collection of particles One important realization that has already emerged is that the way we think about resistance (or dissipation in general) in these systems must be altered to include the possibility of electrons traversing the entire sample with little or no voltage drop—zero resistance! By investigating the size dependence and temperature dependence, we can determine how a quantum system evolves into the more familiar classical system This allows a slightly different probe of the correspondence principle, where instead of letting $\hbar$ tend to zero, we may directly observe the averaging which leads to much of classical physics

The wavefunction of each electron comprises two parts amplitude $C(r)$ and phase ϕ, $\Psi = C(r)\exp(i\phi)$ The quantum interference among electrons which have travelled through the sample via all the various conduction paths available in a device has been observed directly in recent experiments at very low temperatures Electrons might enter the device in phase, but upon reaching the other end, have been phase-shifted relative to

each other because of collisions with defects along the way If phase memory is maintained [2, 3] along each path, then the current exiting the device is a superposition of the wavefunctions in all of the paths Moreover, the amplitude of the superposed wavefunction is determined by the defect configuration, because it is the details of the defect scattering that cause the wavefunction to acquire a particular phase shift

A magnetic field can be used to tune the phase of the electronic wavefunction An intriguing result of the relation between the wavefunction and the magnetic vector potential **A** (the relationship, loosely speaking, is the quantum-mechanical analogue of the Lorentz force) was pointed out by Aharonov and Bohm in 1959 [4] If upon completing some path **s** the phase of the wavefunction is changed by δ_0, then when the path encircles a magnetic flux Φ, $\delta_0 = \pm(e/\hbar)\int \mathbf{A}\cdot d\mathbf{s}$ (where the sign of the correction depends on whether the electron circulated clockwise or anticlockwise around the fluxoid) This is true even if the magnetic field is completely confined to the interior of the path so that the electron always travels in a magnetic-field-free region The existence of a vector potential **A** is all that is required to produce the phase shift Using this relation and the 2π symmetry of the wavefunction [5], Aharonov and Bohm showed that, if a beam of electrons split around a fluxoid and then recombine (see figure 1), the resulting current would be modulated periodically by the amount of flux The modulation results from the alternating constructive and destructive interference between the electrons from the two beams as the vector potential associated with the fluxoid shifts the wavefunction phases For each additional flux $\Phi_0 = h/e$, there would be one complete cycle in the intensity of the current

The coherence of the electron wavefunction is a crucial requirement for the observation of oscillations in current If the phases of the wavefunctions become scrambled before the split beam recombines and is detected, then the periodic oscillations are washed out The smooth tuning of the phases provided by the magnetic field is lost in the random changes of phase suffered when the beam becomes incoherent The principal question to have been settled by the experiments is whether or not the scattering that is inherent in transport in real condensed-matter systems is enough to scramble the electron wavefunction phases

In the following, the material will be presented roughly in the historical order in which it arose Although this approach sacrifices standard pedagogic methods, it serves to make the tale of the scientific venture more accurate In §§ 2 and 3, background is set by discussing the physics of the Aharonov-Bohm effect and by describing the effects of wavefunction coherence on electrical conductance The modern impetus to the searches for Aharonov Bohm oscillations in conductance was an experiment by

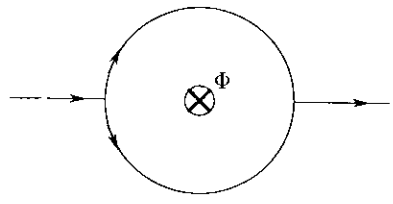

Figure 1 Schematic illustration of the geometry which results in periodic Aharonov Bohm oscillations A coherent beam enters from the left, splits around a magnetic flux Φ and recombines The intensity of the current exiting to the right oscillates with period h/e

Sharvin and Sharvin which discovered oscillations of period $h/2e$ in the resistance of a cylinder This is reviewed in § 4 Sections 5 and 6 recount the theoretical studies which sprang up from that experiment and which predicted a different result, namely that the period of oscillation in a single loop should be h/e In §§ 7 and 8, the story of the experimental confirmation of the h/e oscillations and the discovery of random conductance fluctuations is retold, and some of the phenomenology of the fluctuations is discussed Section 9 contains a brief review of the perturbation theory which is relevant to coherent transport Various averaging mechanisms are described in §§ 10, 11 and 12 Preliminary results on the effects of magnetic impurities are described in § 13 A brief review of some of the interesting and important experiments on semiconducting materials is given in § 14 The explanation of why both the h/e and aperiodic fluctuations are asymmetric with respect to magnetic field direction is detailed in § 15 In § 16 it is noted that significant discrepancies occur between the predictions from perturbation theory and the experiment The observation of non-local voltage fluctuations in small devices is described The theoretical predictions concerning the possible observation of Josephson-like effects in small normal metal structures are reviewed in § 17 Finally, in § 18, some concluding remarks are made about a few of the remaining questions in the field

2. The Aharonov–Bohm effect

There are two points which make up the essential physics of the Aharonov–Bohm effect [4] The first point is that the electron wavefunction is single-valued everywhere in space and has period 2π [5], and that $\int \mathbf{A} \cdot \mathbf{ds}$ adds directly to the phase of the wavefunction The wavefunction of an electron encircling a magnetic flux acquires an additional phase $\delta = (e/\hbar)\int \mathbf{A} \cdot \mathbf{ds}$ (By the usual definitions in electrostatics, the flux Φ is the magnetic intensity $\mathbf{B}$ in an area L^2, and the magnetic intensity $\mathbf{B} = \nabla \times \mathbf{A}$) If a beam of electrons is split around a magnetic flux and then recombined (see figure 1), the resulting superposition of the electrons in the combined beam will exhibit amplitude oscillations The oscillations will be periodic in the magnetic flux, the period being $\Delta\Phi = \Phi_0 = h/e$ because Φ_0 is the amount of flux required to enforce a 2π relative phase shift between the split beams † The second criterion is that the wavefunction retain phase memory throughout the splitting, recombining and measurement of the superposition amplitude Any scattering events that randomize the phases of the wavefunctions in the beam would, therefore, wash-out the oscillations in the superposed amplitude It is worthwhile to note that, in the geometry of figure 1, the magnetic field H is physically separate from the wavefunction This spatial separation of the wavefunction and the field implies, in the framework of classical physics, that there can be no effect on the particle represented by the wavefunction From this argument, the Aharonov–Bohm effect is said to prove that the magnetic vector potential is a real physical potential, not simply a mathematical convenience

Observations of the Aharonov–Bohm effect date back to the early 1960s Within a year of the publication of Aharonov and Bohm's first paper on this subject, Chambers [7] reported an electron-beam experiment in which a standard electron microscope

† It is interesting to note that, somewhat earlier, Ehrenberg and Siday [6] had arrived at the same conclusion using only the uniqueness of the index of refraction and the de Broglie construction

was converted into an interferometer The experimental arrangement was similar to that shown in figure 1 with the addition of two types of magnetic field source The first was a Helmholtz magnet which provided a uniform field along both branches of the beam The application of this field produced no noticeable effect on the interference pattern The second field was produced by an iron whisker 1 μm in diameter and 0 5 mm long, located in the centre of the split beam path As the position of the whisker was changed, the interference pattern changed in the way predicted It was argued that the change in the pattern could not be due to any leakage flux, but depended only upon the total amount of flux contained within the whisker Thus an effect which depended solely upon the existence of a vector potential was apparently confirmed The same oscillations in vacuum have been observed recently using more sophisticated methods [8, 9], wherein magnetic flux was completely confined to the region between the paths by superconducting shields [9] These experiments confirmed the Aharonov–Bohm effect in vacuum and proved the physical existence of the vector potential **A** Aharonov–Bohm oscillations have also been observed in superconductors [10–12] and in single crystals of bismuth [13] In all of these cases, however, there is essentially *no scattering* nothing which might destroy the electron's phase coherence

The conduction process in normal metals is very different In a metal, the electron diffuses its trajectory is a random walk The electron scatters elastically from obstacles such as lattice defects, impurity atoms, boundaries between grains of metal forming the device, and so on (collectively referred to as impurity scattering), as it diffuses through the sample For more than twenty years, theoretical physicists have argued as to whether or not such momentum scattering would prevent the observation of the Aharonov Bohm oscillations By far, the dominant opinion was that the impurity scattering *would* destroy the oscillations [14, 15] A small group [16–18] of theoreticians have maintained instead that only *inelastic* scattering (which changes the energy state of the electron) destroys the oscillations, and it is these few who have been vindicated by the recent experiments [19–21]

3 Conductance in disordered systems: phase coherence and Landauer's formula

In the canonical version of the Aharonov–Bohm experiment, the wavefunction propagates as a free particle (a plane wave) The diffusive motion of an electron in a metal is *not* the same situation at all The electron's trajectory is a random walk with an average step length l (One may instead assume an average collision rate $1/\tau$, and that the mean free path length is the product of the Fermi speed and the mean time between collisions, $l = v_F\tau$) Mean free paths in common metals depend strongly on the cleanliness of the material and the quality of the crystal that form the wire In materials that have many lattice defects, for instance, chemical impurities, vacancies or grains, the mean free path is usually of the order of the average distance between scattering sites Typically in metals prepared by standard methods, this length is only a few nanometres or a few tens of nanometres The motion of the electron in the metal is, therefore, in the opposite limit it scatters very frequently, since the size of device is large compared with the mean free path length, $l \ll L$

By analogy to Shubnikov de Haas theory [22], it was believed that elastic scattering would mix the energy levels, so that the Dingle factor $\exp(-\hbar/\tau\Delta E)$ would damp the oscillation amplitude [14, 15] (Here ΔE is the separation of the individual energy levels in the conduction band and τ is mean free time) This is certainly true of any effects that result from shifts in the energy levels of the device, as shown by Dingle

himself [23] To illustrate just how damaging this exponential is in an experiment, suppose that we study a gold wire, 50 nm in diameter and 500 nm long, which has a resistance $R = 10\,\Omega$ In this altogether typical example, $\Delta E \sim 10^{-27}$ J and $\tau \sim 10^{-14}$ s so that $h/\Delta E\,\tau \simeq 10^{6}$, and the oscillation amplitude is completely destroyed

A second important problem is that of finite temperature At first thought, one would have expected that if the thermal energy is larger than the energy spacing between levels, $k_B T > \Delta E$, the quantum interference existing over the whole device would be destroyed For the previous example, the temperature would have to be below 10^{-4} K in order for thermal smearing to be unimportant This temperature is inversely proportional to the volume of the system, so it would appear hopeless to attempt to observe any relative of the Aharonov–Bohm effect in a sample of reasonable size Fortunately, this thermal smearing effect is not as severe as this estimate might suggest and will be discussed in detail later

A minority [16, 17] held that such momentum relaxation was irrelevant that only *inelastic* scattering would destroy the electrons' phase coherence One of the earliest demonstrations of this followed from Landauer's work on the fundamental sources of the electrical resistance arising from disorder Consider the strictly one-dimensional model of conductance illustrated in figure 2 Electrons of energy $E = \mu_i$ arrive from the left-hand reservoir, are transmitted through the random potential (which scatters only elastically) with probability t and reflected back with probability $1-t$ Upon calculating the current from left to right for a potential difference $\mu_f - \mu_i$, Landauer found that the conductance G of the sample was a simple function of the transmission probability of the disordered region [2, 3], namely

$$G = \frac{2e^2}{h}\,\frac{t}{1-t}, \tag{3 1}$$

where e is the magnitude of the charge carried by an electron, h is Planck's constant and the factor of two accounts for the spin degeneracy of the electrons In his analysis, he noted that the transmission through the disordered region is reversible In fact, it was necessary to enforce phase relaxation of the wavefunction (incoherence) *in the reservoirs* in order to ensure the positive resistance of the device (The infusion and extraction of carriers into and from the system is required, otherwise no dissipation (resistance) occurs [24]) This was done by thermalizing the electrons in reservoirs on

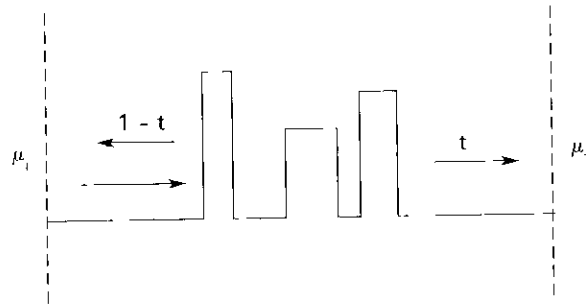

Figure 2 The model used by Landauer to calculate conductance of a random one-dimensional potential A random potential lies between two infinite reservoirs which supply (μ_i) and sink (μ_f) carriers A current (unit intensity) enters from the left and is reflected or transmitted with probability $1 - t$ or t, respectively

either side of the disordered region In the absence of such reservoirs, however, the reversibility of the transmission through the disorder implies that the electron wavefunction retains phase memory, i e the phase shifts introduced by the elastic collisions (momentum relaxation) with impurities do *not* prevent phase coherence [25]

This difference between elastic and inelastic scattering is crucial In polycrystalline metals, though the mean free path (the average distance travelled between collisions with impurities) l is seldom longer than a few hundred ångstrom, the distance over which the electron retains phase memory L_ϕ (the distance between inelastic collisions or other phase-randomizing events) can be as much as a few microns The random walk which the electron undergoes while traversing the sample *does not destroy its phase memory* Although the particle scatters into a new momentum state, the phase of the wavefunction is changed deterministically We are, therefore, using the word 'coherence' a bit loosely Usually a wave that propagates freely is said to have coherence along the wave In contrast, the electrons in a metal scatter frequently, but since the collisions are elastic (i e reversible) all of the electrons that traverse a particular path (collide with the same impurities) arrive in phase they are coherent with each other (but randomly shifted from a plane wave from the origin to the terminus of the path) On the basis of this understanding, Landauer suggested that in a clean normal metal at low temperatures one might be able to see some effects associated with long-range phase coherence [16]

4. Experiments on large samples: observation of $h/2e$

The debate as to whether or not momentum relaxation would prevent the observation of Aharonov–Bohm oscillations in metals was entirely theoretical until 1981 In that year, Sharvin and Sharvin [26] observed field-periodic oscillations in the resistance of a Mg cylinder (approximately 1 μm in diameter and 1 cm long) in an axial magnetic field Moreover, the observed oscillations were periodic in $\Delta\Phi = h/2e$, half the normal Aharonov–Bohm period Although startling to many of us because of the extra factor of 2 in the period, the results were, including the detailed shape of the oscillations, in quantitative agreement [27] with theoretical predictions made several months earlier by Al'tshuler, Aronov and Spivak (AAS) [15] who applied the mathematical techniques developed to describe weak localization [28] in doubly connected structures (i e loops and cylinders without leads)

In these experiments, the basic physics is that the electron trajectory around the cylinder has some probability of returning to its point of origin If quantum-mechanical phase coherence is maintained, then pairs of paths which are the time-reversal of each other (illustrated in figure 3) strongly enhance the likelihood of return to the origin [29–31] One naive way of stating this is that the interference is between two different electrons which start at the same point, travel in opposite directions around the cylinder, but scatter off from exactly the same impurities and interfere back at the origin Because of their formal resemblance to superconducting Cooper pairs [32], these time-reversed pairs are referred to as 'Cooperons' It is this enhancement that has been widely studied in metallic systems under the name of 'weak localization' (For this purpose, 'metallic' means that $G > e^2/h$, it has nothing to do with the chemical composition of the sample) The decreasing frequency of inelastic scattering events as the temperature tends to zero absolute allows the contribution of ever larger time-reversed paths, and since the electron is spending more time at the origin, this increases the resistance of the sample (This increase has been intensively studied in two dimensions [33, 34], where the resistance increases logarithmically as the temperature

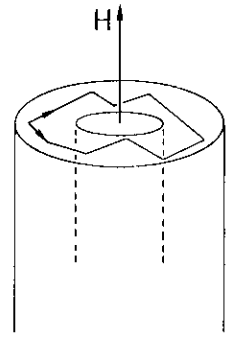

Figure 3 Schematic illustration of the cylinder experiment and the time-reversed pairs of trajectories which give rise to the AAS oscillations in the presence of an axial magnetic field H

decreases, and several excellent reviews of the theory exist [34 38]) Upon confining such pairs of time-reversed trajectories to a loop that encircled a magnetic flux, it was noted that the pair effectively encircled $2\Phi_0$ (see figure 3) It was simply this factor of 2 which appears in the period of oscillation observed in the cylinder experiments (One final point note that as AAS considered only time-reversed *pairs*, they were ignoring the processes that can give rise to the normal period h/e They justified this negligence using Dingle's argument [14, 15])

We emphasize here that the experiment by Sharvin and Sharvin was the first clear observation of an Aharonov Bohm effect in disordered material The mean free path in these experiments is very short about one hundred times smaller than the circumference of the cylinder The electron on average will experience about 10^4 collisions before returning to the origin These experiments prove that elastic scattering does not destroy the phase memory of the electrons (A similar observation had been made some years earlier in Al cylinders far above the superconducting critical temperature, but at that time the oscillations were assumed to be the result of superconducting fluctuations [39])

After the observations by Sharvin and Sharvin, several groups repeated the cylinder experiment and confirmed the presence of the $h/2e$ oscillations, as well as the absence of any h/e oscillation [27, 40 43] Some typical data from the experiments of Gijs *et al* are shown in figure 4 In all of the experiments, the oscillation amplitude, shape and decay with increasing magnetic field were in *quantitative* agreement with the theory [40] Upon enforcing the boundary conditions associated with the loop geometry (a ring without leads), the Cooperon contribution to G has the form

$$\Delta G = \frac{e^2 I_1}{2\pi^2 \hbar} \frac{\sinh(L/L_1)}{\cosh(L/L_1) - \cos(2\pi\Phi/\Phi_0)}, \tag{4 1}$$

where†

$$\frac{1}{L_1^2} = \frac{1}{L_\phi^2} + \frac{1}{3}\left(\frac{2\pi w H}{\Phi_0}\right)^2 \tag{4 2}$$

† Strictly speaking, the unit tesla refers to magnetic induction, conventionally denoted by B In this work, however, our convention will be to use the unit tesla for magnetic field, $H = B/\mu_0$, since the SI unit for field (Amp turn m $^{-1}$) is unwieldy

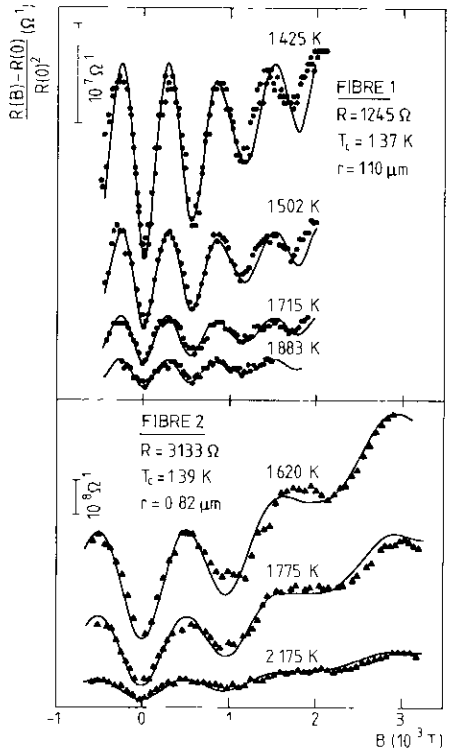

Figure 4 Aharonov–Bohm conductance oscillations with period $h/2e$ observed in two Mg cylinders at several temperatures by Gijs *et al* [42] The solid lines are fits (using L_ϕ as an adjustable parameter) to the AAS theory [15]

In equation (4 2), w is the width of the wires forming the loop, in other words, the thickness of the cylinder The only free parameters in the theory are L_ϕ and the radius of the cylinder, both of these can be determined from other experiments so that, in principle, the theory can be properly compared to the experiment, i e not adjusted to fit The solid curves in figure 4 are examples of how beautifully this theory describes the data at each temperature (In this analysis, however, L_ϕ was fitted and not independently determined) A variation on the experimental method involving large two-dimensional arrays of loops instead of cylinders found the same dominant $h/2e$ period [44–47] Theoretical analysis of a two-dimensional network which followed the work of AAS proved that the coherent backscattering could also quantitatively describe the oscillations in arrays [48]

5. Conductance of a one-dimensional loop

There were two early qualitative discussions [16, 17] which suggested that the oscillations might not be destroyed by elastic scattering, but solid theoretical evidence that the elastic scattering was benign was presented only very recently There have been three methods used to determine the existence of the expected conductance oscillations One approach is to solve for the conductance of the device by direct calculation of the

quantum-mechanical transmission coefficient of the sample [18] The second (historically) method was numerical simulation [49], and most recently, a form of Green-function perturbation theory has been applied with surprising results [50–52]

In 1983, it was shown that an isolated strictly one-dimensional disordered loop (closed chain of atoms) exhibits energy oscillations as the flux threading the loop changes [53] The period of the oscillations is h/e (Earlier work [54, 55] addressing flux quantization in hollow superconductors had noted that all extrinsic properties oscillated with period Φ_0) The model maps onto the elementary case of a one-dimensional lattice where the magnetic flux replaces the lattice vector (see figure 5) Following a marker around the loop corresponds to traversing the unit cell of a perfect one dimensional crystal The energy oscillations are an indication that the properties of a disordered ring might also oscillate with period h/e, but in the absence of irreversibility, the relevance to the resistance of a loop with leads was not demonstrated (The importance of this distinction has been the subject of several works [24, 56–59] The closed system stores energy, but cannot dissipate the energy an open system dissipates the energy when the carriers leave the system [56] The closed system does not have resistance, properly speaking -the flux of carriers through the device is necessary for resistance to occur [24]) Several other authors have also studied the one-dimensional loop [60], mostly with an eye toward explaining the Sharvin–Sharvin experiments [61–64] The next iteration of the model was to add one-dimensional leads to either side of the loop as illustrated in figure 6 (*a*) [65–67] The overall transmission amplitude for the leads plus loop was calculated by brute algebra, and it was found to oscillate periodically with h/e, which by Landauer's formula, implies that the resistance oscillates Moreover, the relative amplitude of the oscillations in G was predicted to be $\Delta G/G_0 \sim 1$ (G_0 is the average conductance of the sample)

One subtle point was also noted in this early work The details of the oscillation amplitude and the phase of the oscillations were dependent upon the choice of impurity configuration (i e on the values of t_1 and t_2) It was discovered that the oscillations

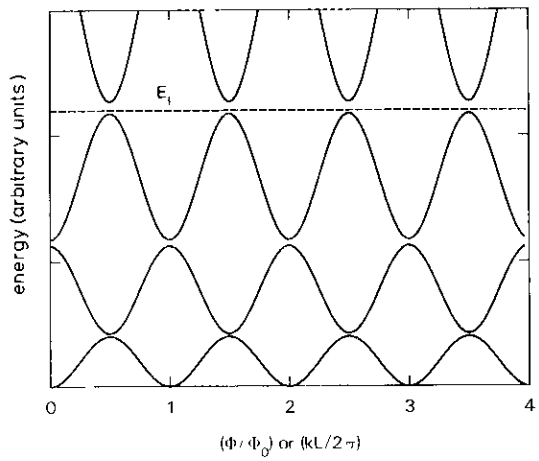

Figure 5 Schematic illustration of the energy bands in a one-dimensional loop Depending on the model, the abscissa might represent the lattice vector k (repeated-zone scheme) or the magnetic flux Φ (closed loop with Aharonov–Bohm flux) The Fermi level is schematically indicated by the dashed line

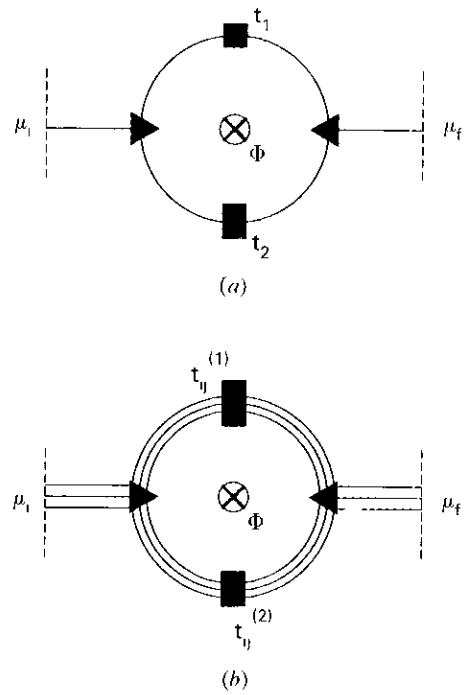

Figure 6 (*a*) Schematic picture of the disordered one-dimensional loop, with one-dimensional leads connected to reservoirs μ_i and μ_f The scatterers t_1 and t_2 represent the disorder in the arms of the ring (*b*) The multichannel ring geometry The matric t_{ij} is the transmission coefficient mixing the various transverse channels in the arms of the loop The triangles at the nodes of the loops represent ideal beam splitters [69]

could be either a maximum or a minimum in resistance at zero magnetic field, and would vary from sample to sample because the microscopic location of scattering centres would vary between nominally identical samples We re-iterate for emphasis the resistance of a given device might be either maximum or minimum at zero magnetic field depending on the details of the scattering in *that particular device* In a different device with another impurity configuration the oscillations might have the opposite polarity The period of oscillation, however, is always h/e

The difference between the results obtained for a ring using the Landauer formula and the weak-localization theory can be understood by realizing that the conventional approach to transport calculations (including the weak-localization calculations) is to ensemble average over all possible impurity configurations The only quantum corrections to the conductance which survive this approach are the Cooperon contributions All sample-specific contributions, such as those considered here, are averaged to zero In all the experiments up until that data, the overall size of the devices were rather large, $L \sim 1\ \text{mm} \gg L_\phi$ Because of the random polarity, Gefen noticed that the amplitude of the h/e oscillations would average to zero in large samples (Y Gefen, private communication, [68]) The polarity is unique only over distances of the order of the phase coherence length L_ϕ In samples which are much larger than L_ϕ, the polarity of the h/e oscillations is not correlated in regions of the sample that are separated by

more than L_ϕ When these uncorrelated regions are averaged to form the overall resistance of the device, the amplitude of the h/e oscillations is reduced (presumably to zero) in cylinders and very large arrays

6 The conductance formula for many channels

After the prediction of h/e oscillations in one-dimensional loops, an important question was posed Will the h/e oscillations survive in a real sample of finite width and thickness? The one-dimensional loop is an extremely idealized model of a real wire with many parallel channels over which the conduction paths are distributed The averaging caused by scattering among these channels might still destroy the oscillations in any practicable measurement

The more realistic model (figure 6(*b*)) containing N parallel momentum channels was solved for the loop geometry [69] A new conductance formula was derived, again, by direct calculation of the transmission coefficient [69, 70],

$$g=\frac{h}{2e^2}G=\frac{\left(2\sum_i t_i\right)\left(\sum_i v_i^{-1}\right)}{\sum_i[(1+r_i-t_i)v_i^{-1}]}, \tag{6 1}$$

where $t_i(r_i)$ represent the total transmission (reflection) of current into channel i and v_i is the velocity ($\hbar k_i/m$) of the carriers in the ith channel The sum extends over a maximum of $N=Sk_F^2$ transverse momentum channels, where S is the cross-sectional area of the wire, and k_F is the wavenumber at the Fermi surface The reasoning in support of this conductance formula for many channels is quite subtle and still somewhat controversial (P A Lee, private communication) It assumes idealized voltage probes [71] which are not easily fabricated in a real device In the limit $l\ll L$ (fairly strong scattering), however, it reduces to the widely accepted formula [72]

$$g=\mathrm{Tr}\{\mathbf{t}\mathbf{t}^\dagger\}, \tag{6 2}$$

where the matrix $\mathbf{t}$ describes the transmission across the disordered region Very recently [73], it has become clear that the fundamental difference between the two versions of the conductance formula is not the condition $l\ll L$, but rather that equation (6 1) assumes an idealized four-probe measurement, and $g=\mathrm{Tr}\{\mathbf{t}\mathbf{t}^\dagger\}$ assumes an idealized two-probe measurement In the first case, the voltage drop across the device is measured by 'ideal potentiometers' which are some distance from the points at which the carriers thermalize (say, just outside the triangles in figure 6(*b*)) In equation (6 2) it is assumed that the chemical potentials (voltages) are measured at the points where the carriers reach thermal equilibrium with the environment

No matter which detailed form of the many-channel conductance formula one accepts, one finds that the conductance g of the multi-channel loop oscillates

$$g=A+B\cos\alpha+C\cos\left\{\frac{2\pi\Phi}{\Phi_0}-\beta\right\} \tag{6 3}$$

The first term is the classical conductance of the sample The second term is a random number depending on the scattering details, and the third term contains the h/e oscillations It was noted that, if the incoming channels were assumed to be completely uncorrelated, then B and C would be smaller than A by a number of order $1/N$ This lower-bound estimate of the oscillation amplitude was quite discouraging since

it implied the oscillation amplitude would be very small in any available device, $\Delta G/G = \Delta R/R \sim 1/N$. Since in the experimental situation, the number N of transverse channels in a Au wire of thickness $t = 40$ nm and width $w = 40$ nm is $twk_F^2 \gtrsim 10^5$, it was doubtful that the observation could ever be made if the $1/N$ estimate were really true.

7 First experiments on single loops

There was, at least, the encouraging result from the cylinder experiments [40] that Aharonov–Bohm oscillations could be observed on length scales of the order of microns in disordered materials. From this point, the question again arose as to whether or not an experiment on a single loop would reveal the normal period h/e. In 1983, experiments were begun to look for h/e oscillations in very small loops of gold. One of the early devices is shown in figure 7(*a*). The average diameter of the ring is 245 nm, the thickness of the film from which the device is made is 39 nm, and the width of the annulus is 30 nm—the width of the connecting leads being considerably larger, 120 nm. The film was polycrystalline, having grains about 50–100 nm across.

The process for manufacturing this device has been described in detail previously [74], but we summarize it here for the sake of completeness. The devices are fabricated on Si_3N_4 windows which are 100 nm thick. (These are made by growing Si_3N_4 onto a Si wafer, and then etching away the Si from the bottom, leaving a transparent window of Si_3N_4.) A metal film is deposited onto the wafer, generally the metal is Au or some material which resists oxidation. The film is coated with resist, and islands of resist are carved with conventional electron-beam lithography to define contact pads. The resist is developed away leaving the pad areas covered, and the wafer is diced into individual devices. The individual chips are installed into a very high resolution scanning transmission electron microscope (STEM), and the device is drawn by rastering the STEM beam back and forth in the desired pattern. Any hydrocarbon contamination in the chamber is burned onto the surface of the film where the beam strikes, and after enough passes of the beam, this 'contamination resist' forms a mask over the device as illustrated in figure 7(*b*). The unprotected metal is then milled with Ar ions, and finally an O_2 plasma strips away the contamination on the surface of the device. Ideally, one achieves a very fine linewidth (~ 10 nm) metal device of any pattern which can be defined on the computer which steers the STEM.

After Al–Si wires were bonded to the four pads on the device, the device was mounted inside the mixing chamber of a ^{3}He–^{4}He dilution refrigerator. The sample was then cooled to temperatures as low as 0.003 K, and the resistance of the device was measured by an a.c. bridge operated at ~ 200 Hz. As the data in figure 8(*a*) demonstrate, the magnetic field dependence of the resistance was not at all what was expected. Rather than having simple h/e or $h/2e$ periodic oscillations, the resistance appeared to be a random function of magnetic field [75, 76]. The amplitude of these fluctuations at the lowest temperatures was 0.1% of the total resistance. After months of repeated measurements, it was possible to demonstrate that the structure was reproducible as a function of field at constant temperature. It was discovered that, unless great care was exercised, small electrical transients delivered to the device when the room-temperature leads were disconnected and reconnected would change the pattern of the resistance fluctuations. Under controlled circumstances, however, the data were reproducible upon retracing the magnetic field or upon cycling the temperature above 1 K.

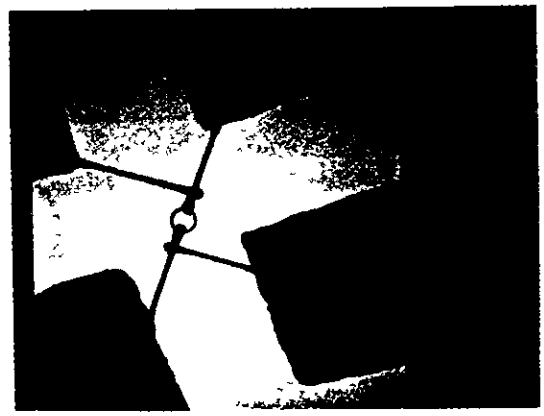

(*a*)

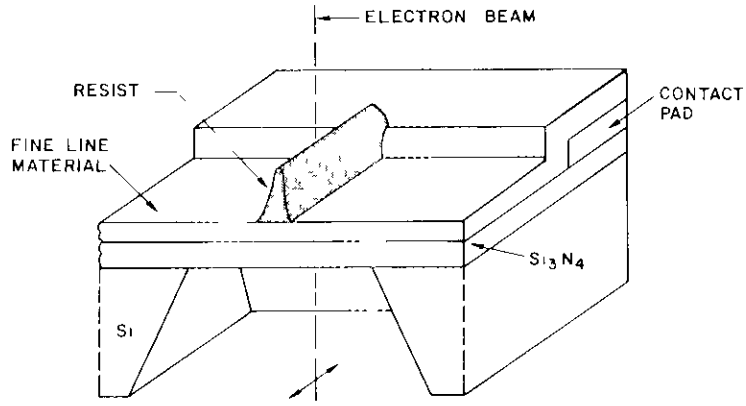

(*b*)

Figure 7 (*a*) Transmission electron photograph of a small Au device The diameter of the loop is about 245 nm, the width of the wires forming the loop is 30 nm, and the width of the leads is ~120 nm The dark areas on the perimeter of the photograph are the edges of the contact pads (*b*) An illustration of the lithographic methods used to manufacture the small devices, showing the film on the undercut wafer covered by the patterned e-beam resist and the contamination resist (darkened material)

Figure 8 (*b*) shows the Fourier transform of the data displayed in figure 8 (*a*) A simple periodic function of magnetic field would appear here as a sharp spike in the Fourier transform at the fundamental frequency of the oscillations The arrows on the figure indicate the expected location of a peak (constrained by the inside and outside diameters of the loop) in the frequency spectrum if either h/e or $h/2e$ oscillations were present in the data Although there is much structure in the transform, there is no clear evidence for the existence of a large single-frequency component The spectrum is as complicated as the raw data itself and, at first viewing, is difficult to interpret

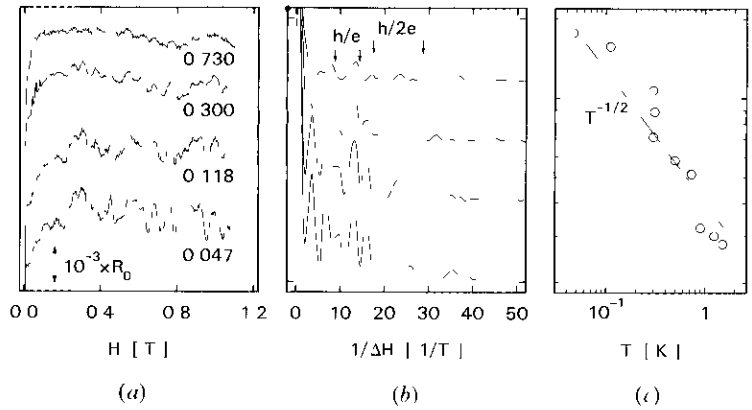

Figure 8 (*a*) The resistance fluctuations measured in the device in figure 7(*a*) at several temperatures (*b*) The Fourier transform of the data in (*a*) (*c*) The height of the peak at $(\Delta H)^{-1}=13\,T^{-1}$ as a function of temperature The vertical scale in (*b*) is arbitrary and linear, and the vertical scale in (*c*) is arbitrary as well

As illustrated in figure 8(*c*), the amplitude of any particular peak in the Fourier transform decreases with increasing temperature, although the positions of the peaks remain more or less unchanged The smaller structure disappears first with increasing temperature, while at higher temperature, only the broad fluctuations are visible The temperature dependence could be approximated by a $T^{-1/2}$ law This form for the temperature dependence was hard to understand, under the altogether reasonable assumption that L_ϕ was larger than the device In this case one expects the magnetic field dependence of the resistance to be positive with a sharp dip near zero field ($H \lesssim 1$ T) and a logarithmic increase at higher field [77] There is, in fact, a dip near $H=0$ in the data, but this was determined to be the result of superconducting proximity effects between the Al wires connected to the device (The temperature dependence of the dip was opposite to what weak localization predicted) In addition, the magnetoresistance at high fields ($H \gtrsim 1$ T) was weakly negative, in contrast to all existing data on Au samples [34] If, on the other hand, L_ϕ were very short, one expects a broad positive magnetoresistance which was not observed, but at least this would explain the absence of the expected periodic oscillations None of these results could be interpreted from the existing theoretical predictions for conductance Furthermore, these fluctuations persisted to very large magnetic fields ($H > 8$ T), in contrast to the weak-localization effects which are destroyed by smaller fields There is a hint from the proximity effect that the mean free path is long, but on balance, there is *no* firm evidence in the data that phase coherence is maintained around the loop

Although understanding of the origin of the fluctuations was poor when they were first reported [78, 79], it began to blossom shortly thereafter Imry suggested that the random fluctuations were the result of an Aharonov–Bohm effect caused by the magnetic flux piercing the metal (Y Imry, private communication) Since the electron trajectories in the metal are random walks, the superpositions, which result in periodic oscillations if the flux is confined to the centre of the loop, are random functions of the amount of flux in the metal He also suggested that the wire would exhibit a fluctuation in resistance after a certain amount of flux was added to it, i e that the fluctuations could not be arbitrarily rapid The first attack on the problem was a numerical

simulation by Stone (using a model developed to study weak localization [80]) which exhibited fluctuations which were very reminiscent of the experiments [49] Moreover, the simulations found that there was indeed a characteristic magnetic-field scale for the fluctuations The field scale in the fluctuations was about $2\Phi_0$ through the area of the metal projected normal to the field

Since it was certain that l was much smaller than the sample size, these fluctuations could not have been caused by size quantization of the electron wavefunctions In the case of complete size quantization, the magnetic field shifts the energy levels around and can lead to fluctuations which may not appear periodic Such fluctuations will exist in metal particles that have dimensions of the order of the mean free path [23, 81, 82] The averaging caused by the Dingle factor, however, would destroy the fluctuations in devices as large as that shown in figure 7 (*a*) where $L \gg l$

8 Observation of *h/e* oscillations in single loops

Based on the results of the simulations and upon analysis of the experimental field scales, Stone suggested making a larger loop to improve the aspect ratio of hole area to metal area He predicted that, with a better aspect ratio, the field scales associated with the random fluctuations and with the *h/e* oscillations would be sufficiently disparate that the oscillations would be clearly observed In spite of the possibility of exceeding the phase coherence length of the electrons, such a ring was manufactured (figure 9) with a larger diameter (820 nm), but with comparable width of the wires (40 nm) forming the device A renewed effort was made to minimize the amount of metal between the voltage probes (software to steer the microscope was written by R Koch)

A sample of the data from this ring is displayed in figure 10 (*a*) Needless to say, the prediction was borne out –many oscillations were seen superimposed on the slowly varying random fluctuations The data in figure 10 (*a*) cover a small range of magnetic field containing approximately 25 *h/e* periods The *h/e* oscillations are plainly visible [19] On purely phenomenological grounds, we can claim that these oscillations are quite different from the AAS oscillations seen in long cylinders and large arrays Instead of damping out smoothly in magnetic field, these oscillations appear to be unattenuated by the field Instead of the standard monotonic background magnetoresistance associated with weak localization in the large samples, the fluctuations dominate the background magnetoresistance A beautiful proof of the existence of the *h/e* period lies in the Fourier transform of the magnetoresistance data (figure 10 (*b*)) The average area enclosed by the loop, as measured with an electron microscope, is $\pi r^2 = 5.3 \times 10^{-13}\ \mathrm{m}^2$, implying that $\Delta H[h/e] = \Phi_0/\pi r^2 = 0.0077\ \mathrm{T}$ There is a large peak in the Fourier transform exactly at $1/0.0077\ \mathrm{T} = 130\ \mathrm{T}^{-1}$ as well as smaller peak at the harmonic 'frequency' $(\Delta H)^{-1} = 260\ \mathrm{T}^{-1}$ This was the first clear observation of the *h/e* Aharonov–Bohm oscillations in disordered systems

As mentioned above, these data indicate quite a different physical situation than that which exists in large samples The behaviour of the magnetoconductance over larger ranges of field brings this point home In figure 11 the field scale has expanded to include a few Φ_0 through the metal in the device Several of the aperiodic fluctuations are in evidence Accompanying the random fluctuations is a random modulation of the oscillation amplitude, which fluctuates on about the same magnetic-field scale as the background The envelope which modulates the oscillations also results from the flux in the metal Assigning each parameter in the conductance formula for a multichannel

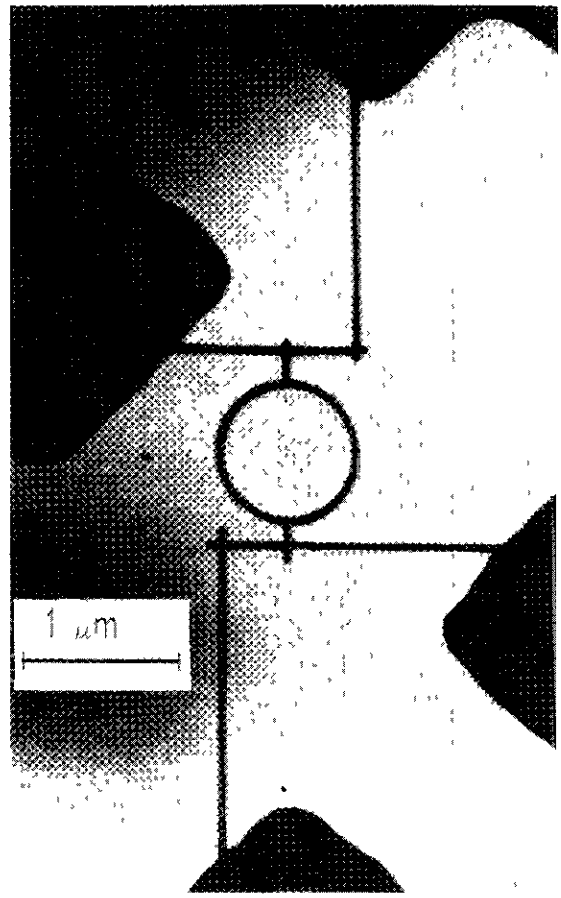

Figure 9 Transmission electron photograph of a large-diameter ring made from 38 nm film of polycrystalline Au, which has a better aspect ratio The diameter is 820 nm and the wires forming the device are about 40 nm across

loop to be a random function of H, one can write the following phenomenological formula (A D Stone and R Landauer, private communications)

$$g(H) = A + B(H)\cos\alpha(H) + C(H)\cos\left\{\frac{2\pi\Phi}{\Phi_0} - \beta(H)\right\}, \tag{8 1}$$

where α, β, B and C are all slowly varying, random functions of H $B(H)$ and $C(H)$ are fluctuations of the background magnetoresistance and the envelope of the oscillations, respectively The random modulation of the oscillation amplitude is a natural consequence of the aperiodic Aharonov–Bohm effects in the wires

The Fourier transform of the data is presented in figure 11 (*b*) In place of the simple peak at $(\Delta H)^{-1} = 130\,\mathrm{T}^{-1}$ seen in figure 10 (*b*), there is a feature which has noticeable width and structure The structure arises from the convolution of the random envelope with the periodic oscillations (A D Stone and R Landauer, private communications) By measuring the areas defined by the inside and outside perimeters of the loop, we can set bounds on the allowable range of h/e frequencies The arrows at the top of the graph

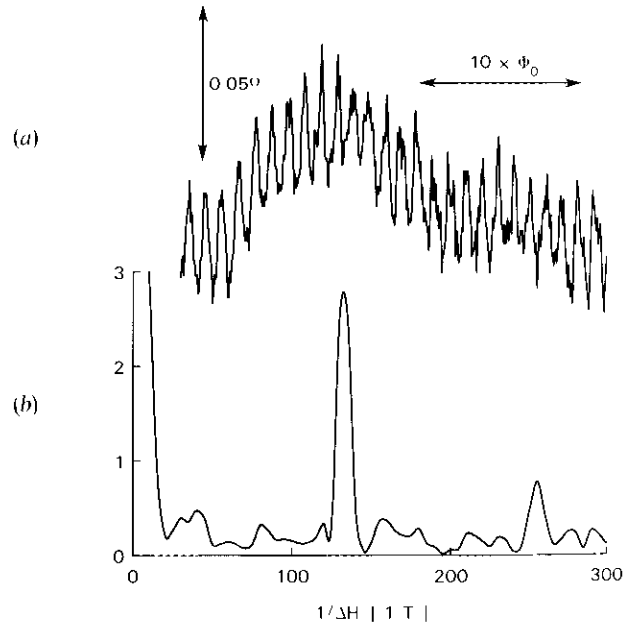

Figure 10 (*a*) The oscillations in the magnetoresistance of the device in figure 9 as a function of magnetic field ($T=0.04$ K) showing the dominant h/e period in the resistance of the loop (*b*) The Fourier transform of the data in (*a*) which contains a large peak at the expected frequency for the h/e ($(\Delta H)^{-1}=130\,T^{-1}$) oscillation and a smaller peak at the harmonic frequency from $2h/e$ ($(\Delta H)^{-1}=260\,T^{-1}$)

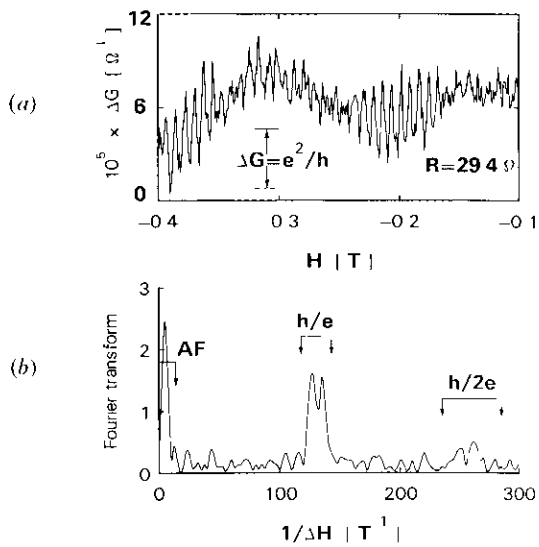

Figure 11 Conductance fluctuations from the device in figure 9 over a range of 0 4 T which illustrates the components of the conductance formula the aperiodic baseline and the random envelope function which modulates the oscillation amplitude Markers indicate the r m s amplitude of fluctuation expected from the conductance fluctuation theory (*b*) The Fourier transform (in arbitrary units) of the data in (*a*) containing structure in the spectral features associated with the various terms in the conductance formula The arrows indicate the allowed ranges of frequency for the aperiodic fluctuations (AF), and for the h/e and $h/2e$ oscillations

indicate these limits, and all of the structure in the Fourier transform fits inside these bounds A similar complexity appears in the $h/2e$ peak There is also a peak near zero frequency which is associated with the random fluctuations in the background magnetoresistance, and the field scale obtained from the simulations, $\Delta H \simeq 2h/e$ through the metal, describes the peak very well

As the magnetic-field scale expands, the oscillations continue without any measurable attenuation A typical sweep from 0–8 T is displayed in figure 12 (*a*) As more of the aperiodic fluctuations are encompassed, the Fourier transform (figure 12 (*b*)) becomes ever richer, but all of the spectral intensity is confined to within the limits set by the device geometry Sweeps of the magnetic field as far as 16 T have revealed no attenuation whatsoever in the oscillation amplitude The aperiodic fluctuations, the h/e oscillations, and the envelope functions retain essentially the same character across the entire field range The AAS oscillations seen in arrays of rings and cylinders were confined to a small region near $H = 0$ mainly because the Cooperon pairs which give rise to these oscillations are destroyed by the field [27, 34, 77] It is clear that the $h/2e$ oscillations are *not* AAS oscillations (equation (4 1)), since the field scale for these oscillations has long since been exceeded in figures 10, 11 and 12 Rather, the observed oscillations are harmonics of the fundamental h/e frequency It is possible that the Aharonov–Bohm oscillations might vanish when Shubnikov de Haas oscillations appear†—when $\omega_c \tau > 1$, where $\hbar\omega_c$ is the energy between Landau levels There is, however, no chance of reaching such a field in normal metal, in the relatively clean gold samples, this would require $H \gtrsim 200$ T

Figure 13 contains data from a somewhat smaller diameter Au loop (diameter 325 nm and linewidth 40 nm) Once again, the oscillations are present The figure displays the resistance up to $H = 5\,5$ T Because of the smaller perimeter, there is some Fourier spectral weight (see figure 13 (*b*)) in the region of $h/3e$ oscillations The difference is that, compared to the 820 nm loop, the field scales associated with the $h/2e$, h/e and random fluctuations are not so widely separated This is simply because the area of the metal between the voltage probes is not much smaller than the area enclosed by the loop Apart from this difference of field scales, all of the qualitative features of the data seen in the larger ring are reproduced

A moment's thought arrives at the principal difficulty in the early experiment on the 245 nm diameter loop The aspect ratio—the ratio of metal area to the area enclosed by the ring—was too small Instead of the one or two Fourier peaks expected for h/e and $h/2e$ periods, these frequencies were interwoven with random fluctuations of nearly the same field scale Since understanding of the random fluctuations was so sketchy at the time of that experiment, the data could not be interpreted as indicating Aharonov–Bohm oscillations With hindsight, however, it is easily seen that the oscillations were indeed present Comparison of the Fourier transform of the resistance of a lone wire

† In fact, experiments on a single-crystal whisker samples of bismuth exhibited h/e flux-periodic oscillation in its resistance a decade or so ago [13] This, however, was *not a disordered material* In those samples, the mean free path was larger than the diameter of the sample The oscillations were size-limited Shubnikov–de Haas oscillations—the maximum Landau orbit was the diameter of the crystal As soon as the field was large enough so that the Landau orbit would fit inside the crystal, the oscillations became the commonly known $1/H$ periodic Shubnikov de Haas oscillations

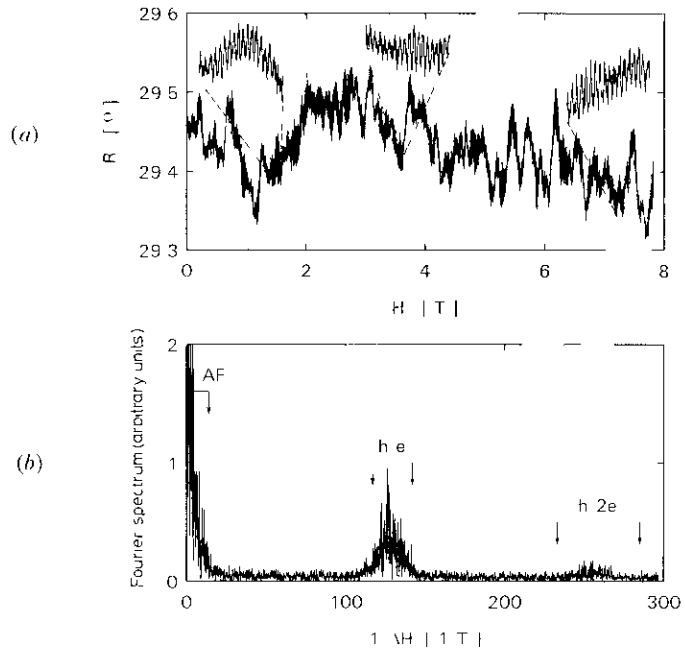

Figure 12 (*a*) The resistance of 820 nm loop covering the range $0 < H < 8$ T As illustrated by the insets, the oscillations are not noticeably attenuated even at the highest fields available (*b*) The Fourier transform of the data in (*a*) which contains spectral density for aperiodic fluctuations *h e* oscillations and *h* 2*e* oscillations

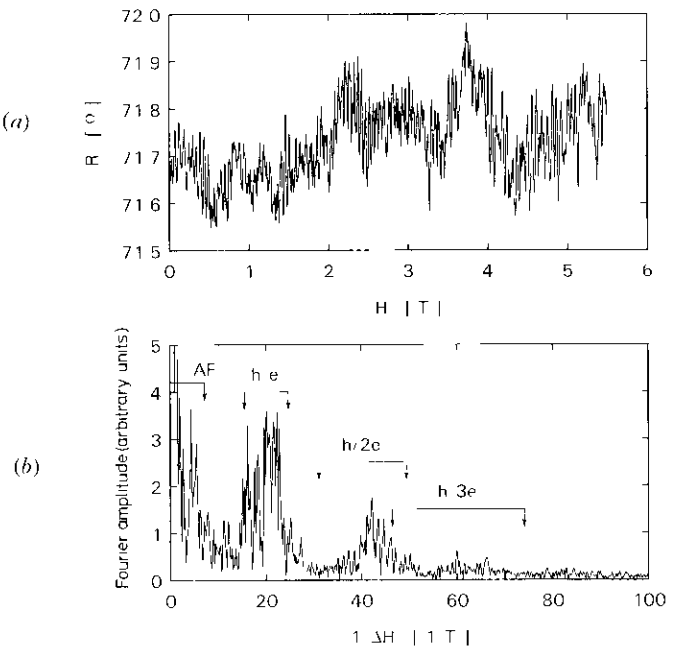

Figure 13 (*a*) Resistance as function of magnetic field strength for the 325 nm diameter loop at $T = 0.06$ K (*b*) The Fourier transform of the resistance data in (*a*), with arrows indicating the various frequency ranges expected for aperiodic fluctuations (AF), h/e, $h/2e$ and $h/3e$ oscillations

(figure 14(*a*) having approximately the same area as one arm of the ring makes this clear The two Fourier transforms are displayed in figure 14(*b*) The spectrum of the wire has no features at frequencies $\Delta H)^{-1} \geqslant 7\,\mathrm{T}^{-1}$ In contrast, the ring spectrum contains several peaks at higher frequencies These peaks lie in the regions of frequency expected for the h/e and $h/2e$ processes, and above the upper limit for the $h/2e$ frequency, the Fourier spectrum tails off These extra peaks were the signature of the h/e and $h/2e$ Aharonov–Bohm oscillations

It was suggested that, in the early experiment, strong coupling to the environment [18, 69] (through the wide connecting leads) might destroy the oscillations by perturbing the coherent states in the ring which actually enclose the flux The data from these three rings are inconsistent with this prediction Even in a loop with very wide leads, the resistance fluctuations are quite strong $\Delta R/R \sim 0\,1\%$, much larger than the $1/N$ estimates [69], where N is the number of channels in the leads, which in figure 7(*a*) is $N \simeq 7 \times 10^5$ The oscillations, then, are *huge* So long as the influence of the environment is not strong enough to destroy the phase coherence, the size of the contacts does not seem to affect the amplitude of the oscillations

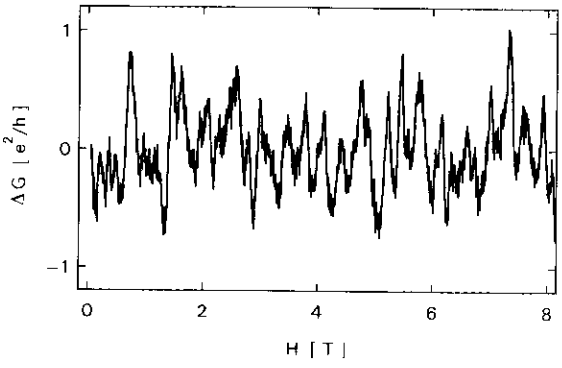

(*a*)

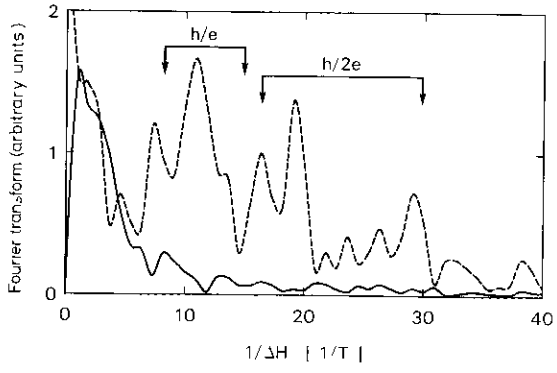

(*b*)

Figure 14 (*a*) Resistance of a single wire 310 nm long and 25 nm wide at $T = 0\,01$ K (*b*) Comparison of the Fourier transform of the wire data in (*a*) (solid line) and the ring data from figure 8(*b*) (dashed line) illustrating the presence of Aharonov–Bohm oscillations outside the field scale associated with the random fluctuations from the wire only

Very shortly after the reports [19, 83–85] of these results, the h/e period was also observed in silver loops [20] These observations in silver loops confirmed much of the phenomenology mentioned above There were, however, two pointedly different results First, the Ag loops exhibited AAS oscillations near $H=0$ which had been conspicuously absent from the Au loop data This absence appears to be universal, in that more than a dozen Au samples have been studied and *none* has exhibited AAS oscillations Second, none of the four Al loops studied [20] exhibited h/e oscillations Above T_c, the data from the Al loops contained AAS oscillations, but no h/e oscillations appeared Neither of these two material-associated discrepancies (the absence of AAS oscillations in Au and the absence of h/e in Al) has been explained satisfactorily Soon after that, an entirely different device exhibited h/e oscillations [21] The device was a double heterostructure (GaAs-$Al_{1-x}Ga_xAs$) oriented so that the field was parallel to the layers --loosely speaking it was a short cylinder The $h/2e$ oscillations were not observed, instead a few h/e oscillations which decayed smoothly with magnetic field were observed At this time, it is not understood why the amplitude of the oscillations should be a monotonically decreasing function of magnetic field in this device It was noted by these authors that nearly all of the disorder in the device was concentrated in the regions where the two layers were interconnected, and that the transport was nearly ballistic in the layers themselves This is quite different from the more homogeneous disorder in the gold and silver loops Even after noticing this difference, however, it is difficult to explain the qualitative differences between the two kinds of experiment One possibility is that the formation of Landau orbits in the high-mobility two-dimensional layers destroyed the h/e oscillations The theoretical conditions are fulfilled ($\omega_c\tau > 1$ and $kT \sim \hbar\omega_c$), but there is no evidence in the conductance for the existence of Shubnikov–de Haas oscillations

9 Universal conductance fluctuations

Within the last year or so, the origin of the aperiodic resistance fluctuations has been attacked through numerical simulation and perturbation theory As mentioned above, Y Imry (private communication) suggested that the magnetic flux piercing the wires in the device might also cause an Aharonov Bohm effect The effect would probably be random (rather than periodic) because the path of the electron is erratic It is not subject to the same geometrical constraint that gives rise to the periodic oscillations, namely there is no well-defined area to enclose an Aharonov–Bohm flux A simulation of a disordered wire [49] (using the method developed to study scaling in the localization problem [80]) found such random fluctuations in the magnetoresistance of the model system The model was very simple, it assigned a potential to each lattice site which was the sum of a random term (representing the disorder caused by impurities and defects) and $e\mathbf{A}/\hbar$ (accounting for a uniform magnetic field) The numerical results for a given arrangement of 'impurities' contained random fluctuations of the resistance versus magnetic field which resembled the aperiodic resistance fluctuations observed in the experiment The model has another intriguing feature The average amplitude of the fluctuations was only weakly dependent on the number of transverse channels The amplitude appeared to follow (at worst) a weak power law in the inverse of the number of channels This result was in direct contradiction with the $1/N$ dependence suggested by the algebraic calculations [69] It was, at least, more consistent with the experiment than the $1/N$ prediction

Based on these hints from the experiments and simulations, an ingenious use of perturbation theory was established by Al'tshuler [50] and independently by Lee and

Stone [51] Until that point, the standard Green function approach had failed to predict any of the h/e or random effects because it contained an ensemble average over the impurity configurations [86] Such an average is certainly not appropriate to a small system having a *particular* configuration of scattering sites which will be reflected in the conductance (Y Gefen, private communication, [68]) The new method allowed the average amplitude of the sample-specific conductance fluctuations and oscillations to be calculated The crux of the argument is that changes in the magnetic field and the Fermi level (larger than some scales) will cause a fluctuation in the conductance which, *on average*, will be the same as the change resulting from a new impurity configuration [51, 87] This permitted the powerful impurity-averaging techniques [88] to be brought to bear on the problem at hand Astoundingly, it was found that the only criterion for the existence of such conductance fluctuations was the coherence of the wavefunction The size of the sample is irrelevant, the fluctuations do not average to zero as the device gets larger, so long as the coherence is maintained (As a technicality, we note that L must be small enough so that quantum coherence occurs in a practicable experiment Typically this limits the sample size to $L \lesssim 10\,\mu$m)

The technique used to obtain ΔG was to calculate the correlation function $F(\Delta E, \Delta H)$ for the conductance,

$$F(\Delta E, \Delta H) = \langle g(E, H) g(E + \Delta E, H + \Delta H) \rangle - \langle g(E, H) \rangle^2, \tag{9 1}$$

where the angle brackets denote ensemble averaging over impurity configurations This correlation function is written as a sum of diagrams such as figure 15 $F(\Delta E, \Delta H)$ is calculated by obtaining the diffusion propagator $P(r, r', \Delta E, \Delta H)$ (e g the upper half of figure 15) by solving the relevant 'diffusion equation'

$$[-i\tau \Delta E + D\tau(-i\nabla + e\Delta A)^2] P(r, r', \Delta E, \Delta H) = \delta(r - r'), \tag{9 2}$$

restricted to the boundary conditions appropriate to a given sample geometry (ΔA is the difference between the two values of A for the two trajectories In place of frequency and vector potential [28], one now has the correlation scales for energy, ΔE, and

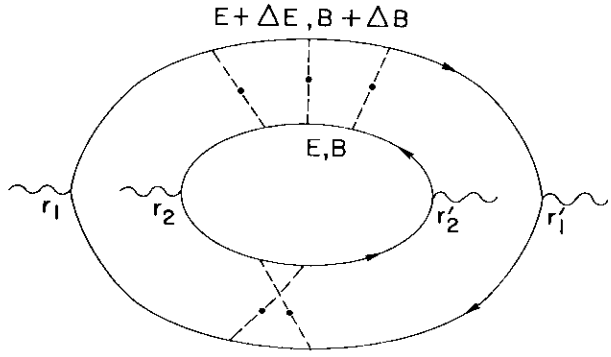

Figure 15 A generic Feynman diagram which contributes to the conductivity correlation function studied by Maldague [87], Al'tshuler [50], and Lee *et al* [51, 52] Current vertices (wavy lines) are connected to each other by electron and hole Green functions (solid lines) which scatter from impurities (dots) Note that the two conductivity bubbles interact with the *same* impurities but at different energies or magnetic fields

magnetic field, $\Delta H = V \times \Delta A$) The impurity ladders (top of figure 15) are summed [37, 38, 86] to give $P(r, r', \Delta E\ \Delta H)$ Note that near zero magnetic field where the Cooperon (the bottom half of figure 15) contributes there is an enhancement of $F(\Delta E, 0)$ by a factor of two Including all permutations on figure 15, they [51] find that so long as phase coherence of the wavefunctions remains, $F(0, 0)$ is independent of length, nearly independent of shape, and of order unity Moreover, it was demonstrated that the fluctuations remain in all physical dimensions † This implies that in *any* quantum-mechanically coherent metallic sample there is a universal amplitude for the conductance fluctuations and oscillations, namely

$$\Delta G = \frac{e^2}{h}\sqrt{F(0,0)} \sim e^2/h \tag{9 3}$$

This result, $\Delta g \sim 1$, is in excellent agreement with the existing experimental data on Au devices as illustrated in figure 11 For instance, the data from figure 8 (*a*) ($T = 0\,046$ K) yield $\Delta G = \Delta R/R^2 = 0\,6\, e^2/h$ It does not describe the data from the near-ballistic samples which exhibit larger oscillations [21]

Imry has proposed one intuitive argument for the size independence of the fluctuations [89 91] He shows that, in a long sample, $L \gg l$, the conductance formula can be represented as the sum over the Lth power of the eigenvalues x_j of products of the transfer matrix (which relates currents on one side of the sample to those on the other side),

$$g \simeq \mathrm{Tr}\,\{\mathbf{t}\mathbf{t}^\dagger\} = \sum_j (x_j)^L \tag{9 4}$$

In this sum, the largest eigenvalues dominate, and the smaller eigenvalues have exponentially smaller contributions to the conductance As the length of the sample increases, the conduction paths associated with smaller eigenvalues no longer contribute to the conductance After arranging the terms of the sum in descending order, eigenvalues smaller than some $x_m \lesssim 1$ become irrelevant (Alternatively one may say that when L exceeds some given length, the paths with $T_i < T_{\min}$ are effectively localized, since $(T_{\min})^L \lesssim 1/e$, and T_i which are smaller than $T_{\min}$ have an exponentially smaller contribution) If the sample length L becomes comparable to the localization length ξ, which describes the decay of the wavefunction to zero, then only the largest eigenvalue x_0 is still contributing to g, and for longer samples [92] ($L > \xi$), the conductance is $g = (x_0)^L \exp(-1/\xi)$ Noting that the eigenvalues are more or less evenly spaced, one can write $x_0 = 1 - \delta$ and $x_j \simeq 1 - j\delta$ so that one obtains $x_m \simeq \exp(-m/\xi)$ The number of surviving eigenvalues m is the number active channels in the device N_{eff} Upon recalling [92], $\xi \simeq Nl$, it follows that

$$N_{\mathrm{eff}} \simeq Nl/L \tag{9 5}$$

The size of the relative fluctuations is $\Delta g/g \sim 1/N_{\mathrm{eff}}$, which implies that $\Delta g \sim L/Nl$ which (by the definition of x_m) is of order unity Very recently, Lee has put forward a

† This is a truly startling result since it also implies that each coherent segment ($L = L_\phi$) of the sample contributes such fluctuations The statistical averaging which destroys the fluctuations in samples containing many incoherent segments is relatively weak -- the amplitude decreases only as $(L/L_\phi)^{-d/2}$ in d dimensions The implication is that the fluctuations will have measurable amplitude, even for rather large objects

complementary argument which starts with the reflection coefficients and arrives at equation (9 5) [93] Imry's physical argument has been tied to the spectral rigidity of the large random matrices which describe the transmission through the disordered region [81, 88, 94–96]

Changes in the magnetic field [51] or the Fermi energy [51, 87] larger than some scale cause changes in conductance which are equivalent to those caused by changes in the impurity configuration The correlation function $F(\Delta E, \Delta H)$ decays on this scale of ΔH or ΔE In one dimension, the energy scale ΔE over which $F(\Delta E, 0)$ decays is (Y Imry, private communication, [51])

$$E_C = \pi^2 \hbar D / L^2 \tag{9 6}$$

This is the sensitivity of the energy levels to the boundary of the device made famous by Thouless in his development of the scaling theory of localization [91] Within a bandwidth E_C, the electron states are spatially correlated, and all of the carriers contribute to the same random pattern of fluctuations in G The particular random function $\Delta G(H)$ depicted in figure 11 is such a fluctuation pattern Changing the Fermi energy by less than E_C has no effect on the pattern of conductance fluctuations, changes of more than this amount would result in the observation of a different pattern of fluctuations, which has the same r m s amplitude The magnetic-field scale for the decay of the correlation function was also calculated and found to be $\Delta\Phi \sim h/e$ through the wire Adding this amount of flux through the device would change the conductance randomly by an amount of order e^2/h (An excellent discussion of the theory of conductance fluctuations has been published recently [52], and many of these results have been derived independently by Al'thsuler *et al* [50, 88, 95 97], Imry *et al* (Y Imry, private communication, [94, 88–100]) and others [101–107]

Surprisingly, it was found that, in two or fewer dimensions, the fluctuation pattern is *critically* dependent upon the placement of the impurities Moving a single impurity farther than approximately one de Broglie wavelength completely rewrites the random pattern $\Delta G(H)$ [97, 104] This extreme sensitivity of G to the individual impurity locations has been invoked to explain the amplitude of the ubiquitous $1/f$ noise seen in metallic films [104]

Extensions of the theory of conductance fluctuations to the case of rings ([108, 109], D Di Vincenzo and D Stone, private communication) predict an r m s h/e oscillation amplitude of $\Delta G = 0\,4e^2/h$ This value depends somewhat on geometrical parameters but the corrections are of order of unity This prediction is in excellent agreement with the observed low-temperature h/e amplitudes For instance, the data in figures 12 and 12 both yield an h/e oscillation amplitude $\Delta G[h/e] = 0\,2\,e^2/h$

The correlation functions extracted from the experimental data on a Au wire 310 nm long and 25 nm wide is compared with the theoretical calculation [52] in figure 16 We emphasize that this is *not* a fit with adjustable parameters Considering the simplicity of the model, the theory is in excellent agreement with the experimental results

10. Energy averaging and correlated energy bands

The temperature dependence of the fluctuations in the more recent experiments is quite complicated [110] In figure 17 (*a*), we display three traces of $R(H)$ at different temperatures On average, the oscillations are large at the lowest temperature and, as the temperature increases, the average oscillation amplitude decreases Viewed locally, the temperature dependence at a particular value of field may not be a smooth function

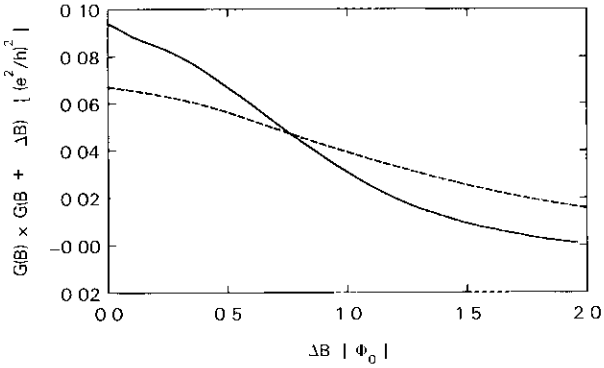

Figure 16 Autocorrelation function in magnetic field of the resistance fluctuations from an Au wire (solid line) The dashed curve is the theoretical calculation [52] for a wire which has an area equal to that covered by the material between the voltage probes in the experiment

of temperature For instance, tracing along the dashed line, at 0 70 K, the oscillations are very small, by 0 20 K, they have grown considerably, but at the lowest temperature, 0 03 K, the oscillations have completely vanished A similar oddity appears in some of the peaks in the Fourier transform Following the dashed line in figure 17 (*b*), at 0 70 K the peak is fairly small, larger at 0 20 K, but has shrunk again by the lowest temperature

The Fourier transform can be reduced one step further to obtain information on the average amplitudes of the various fluctuations as a function of temperature The temperature dependence data in figure 18 are calculated from the Fourier transform by summing the spectral weight across the region allowed by the device geometry, i e from the inside perimeter to the outside perimeter for the oscillations, and over the region Φ_0/L^2 (where L^2 is the area of the metal, projected normal to the field) for the random fluctuations The data are independent of temperature at very low temperatures, and

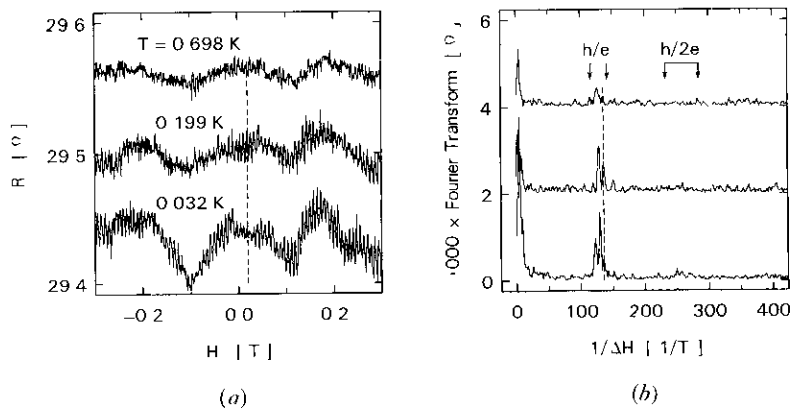

Figure 17 (*a*) The magnetoresistance of the large-diameter (820 nm) loop at three temperatures (*b*) The Fourier transform of the data in (*a*) The dashed lines are included to serve as a guide to the eye as described in the text

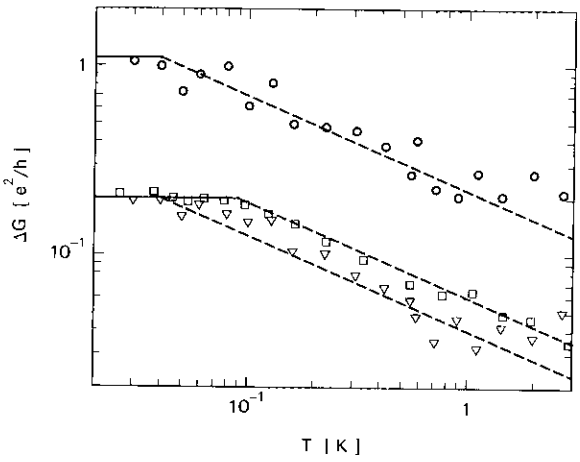

Figure 18 The summed spectral weight of the aperiodic fluctuations (○) and the h/e fluctuations (▽) from the 820 nm diameter ring and the h/e oscillations (□) from the 325 nm diameter ring The solid lines indicate where the data are independent of temperature and the dashed lines depict the $T^{1/2}$ law

fall off as a weak power law, $\Delta G \propto T^{-1/2}$, at higher temperatures The point at which the temperature dependence ceases for the two samples is different by a factor of 2 or so, even though the conductances were measured at the same time and in the same environment

The theoretical explanation of all of these features was developed from the perturbation theory [49, 51, 99] At zero temperature, the impurity configuration in the sample will cause a particular pattern to appear in $G(H)$ Within some bandwidth, it would be expected that the neighbouring levels in the conduction band have spatial correlation and, therefore, generate the *same* pattern in the conductance According to Thouless [92],

$$E_C = G\frac{2\hbar}{e^2}\Delta E, \tag{10 1}$$

where ΔE is the separation between levels in the conduction band This relation, which is equivalent to equation (9 6), gives $E_C/k_B = 0\,085$ K for the 325 nm ring and 0 035 K for the 820 nm ring These numbers are in excellent agreement with the temperatures at which the power law flattens to a constant in figure 18 When $k_B T < E_C$ the fundamental pattern only contributes to the conductance (illustrated by the solid lines in figure 19) In this situation, the averaging ceases in these devices, and this condition is highlighted by the solid lines in figure 18 For $k_B T > E_C$, uncorrelated bands, attended by their own independent fluctuation patterns (dashed lines in figure 19), contribute to the overall (averaged) pattern recorded in the experiment The number of uncorrelated patterns is simply $N = k_B T/E_C$, and therefore the amplitude of the fluctuations in the sum over these patterns is proportional to $N^{-1/2} \propto T^{-1/2}$—precisely the power law determined by the data in figure 18 (dashed lines) We admit that this is a rather naive analysis [49, 51] of complicated physics, but a more careful calculation reproduces this result in one or two dimensions [52]

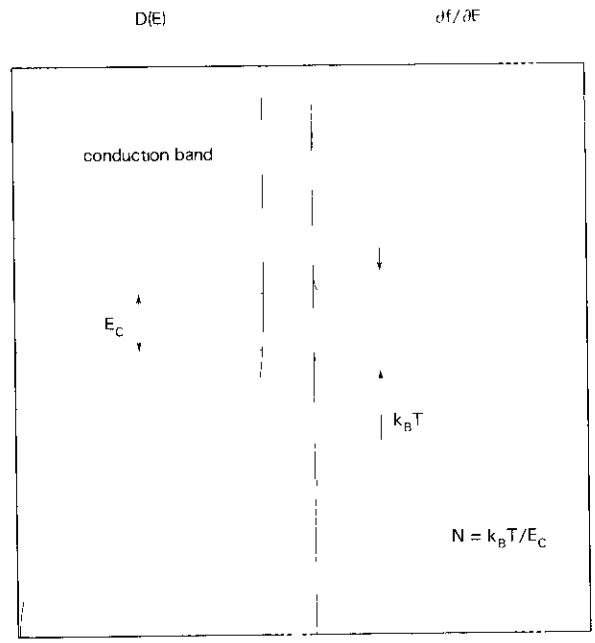

Figure 19 Schematic conduction band $D(E)$ and Fermi surface smearing $\partial f/\partial E$. In the first case (solid lines), $k_BT < E_C$, and only one pattern is represented in the conductance. In the second case (dashed lines), where $k_BT > E_C$, several independent patterns are averaged together.

The non-monotonic temperature dependence in the oscillation amplitude at particular magnetic field values (the dashed line in figure 17(*a*)) can be explained as follows. At the lowest temperature, only the 'fundamental' pattern was being sampled, but as the temperature increased above E_C, more fluctuation patterns began contributing to the conductance. The appearance of oscillations where previously there had been none simply implies that one of the new patterns contained oscillations at that value of H.

11 Small arrays of loops: direct measurement of ensemble averaging

The question as to why the array [44] and cylinder experiments [40] failed to observe h/e oscillations has been settled on heuristic theoretical grounds by the arguments put forward by Gefen (Y. Gefen, private communication, [64, 68, 108]). The experimental determination of the averaging was accomplished in a study of small series arrays of Ag loops [111]. The resistances were measured for arrays containing 1, 3, 10 and 30 loops (see figure 20(*a*)).

Figure 20(*b*) contains some of the raw data from this experiment. The AAS oscillations dominate at these low values of magnetic field in all of the arrays. From the field dependence of the AAS oscillations, it was possible to extract the Cooperon phase coherence length $L_\phi = 2.2\ \mu$m. This length was roughly the separation between the loop centres, which implied that each loop contributed independently to the conductance. At higher fields when the AAS oscillations has been quenched, the h/e period dominated [20, 111].

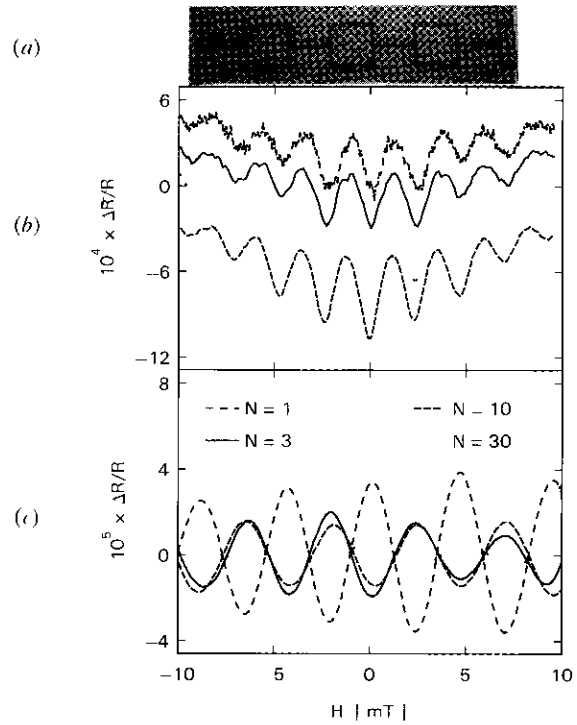

Figure 20 (*a*) Electron micrograph of part of a series array of Ag loops The linewidth is 70 nm and the length of each line segment is 920 nm (*b*) The magnetoresistance of each array at low field illustrating the AAS oscillations (*c*) The data from (*b*) filtered to select the h/e oscillations The polarity of the oscillation at $H=0$ changes from device to device

As predicted by Gefen, the essential point is that the AAS oscillations $\Delta G[h/2e]$ are always maximal (for strong spin orbit scattering [40]) at $H=0$, and the polarity of $\Delta G[h/e]$ is randomly -1 or $+1$ This dichotomy is observed directly in the data from this experiment The AAS oscillations from all of the samples (figure 20(*b*)) have maxima at $H=0$ (as have the AAS oscillations observed in all other published experiments on heavy metals [40] There were also contributions from the h/e process in the vicinity of $H=0$ These can be displayed more clearly by digitally filtering out the random fluctuations and the $h/2e$ processes and leaving only the h/e frequency The filtered data are shown in figure 20(*c*) The first point to note is that the predicted random polarity [68] is indeed observed Two of the samples ($N=1$ and $N=30$) have maxima at $H=0$, while the other two have minima

This random polarity causes the averaging of the h/e period In fact, it is immediately noticed that the oscillation amplitude shrinks as the number of loops increases The explanation is that within each series array the same random polarities appear If the loops add incoherently, then we expect that the average oscillation amplitude is reduced Each phase-coherent segment of the array contributes 'its own' fluctuations with amplitude $\Delta G=\Delta R_s/R_s^2\sim e^2/h$ (R_s is the resistance of the segment) The number of such segments is simply $N=L/L_\phi$ The fluctuations in resistance across the entire array increase as $\Delta R_s=N^{1/2}\Delta R_s$ so that

$$\Delta G=\frac{2e^2}{h}\frac{1}{N^{3/2}}=\frac{2e^2}{h}\left(\frac{L_\phi}{L}\right)^{3/2} \tag{11 1}$$

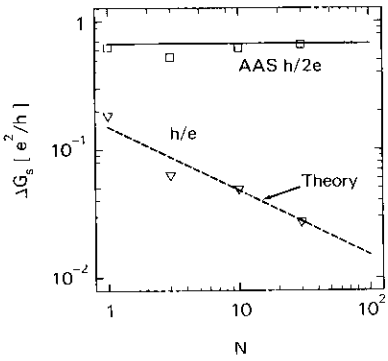

Figure 21 The r m s amplitude of the h/e oscillations and the AAS oscillations (normalized to the resistance of a single loop) as a function of the number of loops The theoretical estimates are obtained from the theory [15 108]

For the purposes of this discussion, it is more illuminating to consider the ΔG fluctuations as normalized to a single loop without connecting leads This removes one factor of N from equation (11 1), and $\Delta G[h/e] \propto N^{-1/2}$ The data in figure 21 yield precisely this result for the h/e oscillations The greater the number of incoherent loops, the smaller the oscillations The AAS oscillations, in contrast, are independent of N In samples containing 10^4–10^6 effectively independent loops [40], the h/e period would be buried in the noise Choosing to study such large samples predetermines that only processes which survive this ensemble averaging can be observed in the experiment The only component of the Aharonov–Bohm conductance fluctuations which survives is the AAS effect, and its preponderance in the cylinders and large arrays is thereby explained

12 The effect of the phase coherence length

All of the above arguments follow from the assumption that phase coherence spans the loop at all temperatures As demonstrated in innumerable experiments studying weak localization [33, 34], L_ϕ consists of a temperature-dependent component L_{in} and temperature-independent components such as magnetic scattering (see the next section) L_s and spin–orbit scattering In the absence of spin orbit scattering we have [34]

$$\frac{1}{L_\phi^2} = \frac{1}{L_{in}^2} + \frac{2}{L_s^2} \tag{12 1}$$

L_{in} is temperature dependent, usually $L_{in} \propto T^{-\alpha}$, where $\frac{1}{2} < \alpha < 2$ The effect on the Aharonov–Bohm oscillations of the shortened phase coherence length which eventually appear at higher temperatures was explored in another experiment [112]

An Sb ring of approximately 900 nm diameter was studied carefully in the temperature range where the inelastic diffusion length was changing The temperature dependence of the inelastic diffusion length $L_{in} = \sqrt{(D\tau_{in})}$ (D is the diffusion constant, and τ_{in} is the mean time between inelastic collisions that destroy the wavefunction phase) can be determined from the magnetoresistance associated with weak localization [34, 77] In the Sb ring, the measured L_{in} followed the usual $T^{-1/2}$ dependence seen in many one-dimensional samples [113] The shortening of L_{in} enforces another

averaging process on the fluctuations This process affects the periodic and aperiodic components differently

The aperiodic components, which result from the effects within a wire, merely 'sense' a shortened sample length Instead of the length L defined by the lithographic pattern, the coherent transport acts only in a region of length L_ϕ, so the wire between the voltage probes contains L/L_ϕ statistically independent coherent devices One result is that the field scale over which the conductance fluctuates increases as the smaller L_ϕ reduces the effective sample size Another results is, of course, that the average amplitude of fluctuations is reduced (see equation (11 1)) because L/L_ϕ statistically independent patterns contribute to the observed fluctuations The periodic components suffer a more destructive averaging The device geometry asserts itself here regardless of whether or not phase coherence is maintained The loss of phase coherence between the nodes of the ring causes an exponential roll-off of the oscillation amplitude $\Delta G \propto \exp(-L/L_\phi)$ because the number of coherent electrons arriving at the terminus of the loop is exponentially reduced

This exponential averaging of the h/e oscillations from the Sb loop is confirmed by the data shown in figure 22 The fluctuation amplitude decays rather slowly and can be fitted by equation (11 1), whereas the h/e amplitude decays exponentially as the temperature decreases By the standard analysis of the weak-localization magnetoresistance (an example of the fit to obtain L_ϕ is given in the inset) the phase coherence length for the Cooperons (the time-reversed pairs which result in localization) was calculated [34, 77] The preliminary results of the fitting procedure yielded $L_s = 0\,76\ \mu m$ and $L_{in} = 0\,26\ \mu m\ T^{-1/2}$ The solid line through the h/e data is

$$\Delta G = \frac{e^2}{h}\left(\frac{2\pi hD}{L_\phi^2 k_B T}\right)^{1/2} \exp(-\pi r/L_\phi) \tag{12 2}$$

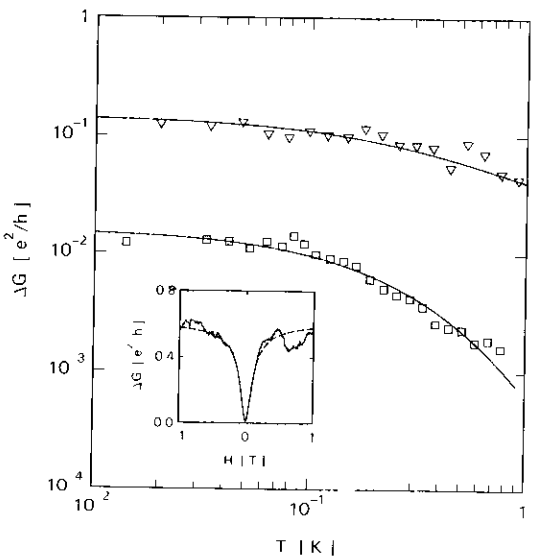

Figure 22 The temperature dependence of the h/e oscillations (□) and aperiodic fluctuations (▽) for an Sb loop having a diameter of 900 nm The solid curves are fits to the data as described in the text The inset is an example of the low-field magnetoresistance and the theoretical fit which determines L_ϕ

The h/e data are described quite well by this curve [112] once it is noted that E_C is larger than $k_B T$ (because Sb is a semimetal and D is quite large) so the quantity in brackets is equal to one In fact, on the sole assumption that the value of L_ϕ determined for the Cooperon describes the single electron, the exponential dependence is confirmed The same value of L_ϕ appears to describe all of the data, and the only adjustable parameter is Δg at $T=0$ From the experiment we obtain $\Delta g=0\,56$ and $\Delta g[h/e]=0\,20$ which is in agreement with theoretical predictions [50, 51, 108] and previous experimental results [110, 111] in other materials

Strictly speaking, all of the theoretical analysis presented so far is valid only for $L_\phi \leqslant L$ This is guaranteed in the Landauer formula (see figure 2) since phase coherence cannot extend into the reservoirs, but in the case of four-probe techniques (see § 16) voltages can be measured at $L<L_\phi$ where this analysis breaks down

13. Effects of magnetic scattering

Spin exchange between the conduction electrons and any paramagnetic impurities in the sample is another source of phase breaking which is familiar in the study of weak localization [34, 77] The coherence of the wavefunction is destroyed when the spin component is randomized, and the superpositions which cause the conductance fluctuations are washed out Scattering from paramagnetic impurities is then expected to destroy the Aharonov Bohm oscillations as well ([52], H Fukuyama, private communication) For strong spin scattering when the spin-exchange rate τ_s^{-1} is very large ($\tau_s^{-1} \simeq \tau^{-1} \gg \tau_{in}^{-1}$), where all of the impurities in the device carry paramagnetic moments, one only needs to consider two regimes At low magnetic field ($g\mu_B H \ll k_B T$), the spins are free to orient themselves randomly, and the spin exchange randomizes the phase of the wavefunction At high fields ($g\mu_B H \gg k_B T$), however, the impurity spins are all aligned with the field as are the conduction-electron spins, and exchange between the two causes no change in the wavefunction In the intermediate region, one can calculate the probability that a spin is aligned with the field

$$S_z = \coth \frac{g\mu_B H}{k_B T} \tag{13 1}$$

In the case of dilute paramagnetic impurities [97] ($N_s \ll N_{imp}, N_s$ is the density of paramagnetic scatterers and N_{imp} is the total density of impurities), the carriers have some reasonable probability of traversing the sample oblivious of spin exchange The calculation of the fluctuation amplitude must then include a reduction of τ_s^{-1}, which accounts for the smaller probability that an exchange will occur (Kondo interactions and spin glasses [97] are further complications which we ignore for the moment) Not only must one include the probability of the spin being paramagnetic, but also the probability of the carrier encountering such an impurity At a particular value of field, this can be accommodated by simply renormalizing L_s (the diffusion length between spin flips), but if one wishes to describe the entire parameter space (N_s, H, T) a more sophisticated model must be invoked [114] The model predicts that for a given density of magentic impurities one obtains an amplitude of the oscillations

$$\Delta G[h/e] - (e^2/h)\coth(g\mu_B H/k_B T)$$

with the 'g-factor' renormalized to account for the matrix element for spin exchange and the dilution of paramagnetic spins Thus, for a given sample with its fixed impurity population, one expects that in the region near $H=0$ the oscillations are quenched by

spin exchange, this region will gradually widen as T increases This is precisely what an experiment finds [114] First, a sample was measured to ensure that there were h/e oscillations throughout the field range Then a small concentration of paramagnetic impurities was adsorbed onto the surface of the device, and the fluctuations were remeasured Figure 23 (a) contains data for $\Delta G[h/e]$ from this Au loop at three temperatures At the lowest temperature (near-zero magnetic field where the impurity spins are free to rotate), the amplitude of the oscillations is zero to within the noise in the measurement, but as the field increases and the spins begin to align, the amplitude increases and eventually recovers the expected value $\Delta G[h/e] \simeq e^2/h$ The value of N_s (the effective g-factor) is undetermined in this experiment, but was fitted to the lowest temperature data This value of g then explains *all* of the data at higher temperatures (see figure 23 (a))

The electron trajectories which result in the $h/2e$ oscillations are about twice as long as those for the h/e oscillation Since the trajectories are diffusive, one would expect that the effective g-factor for these oscillations would be larger by a factor of about 4, fewer of the electrons survive without destroying their spins An experimental test [114] of

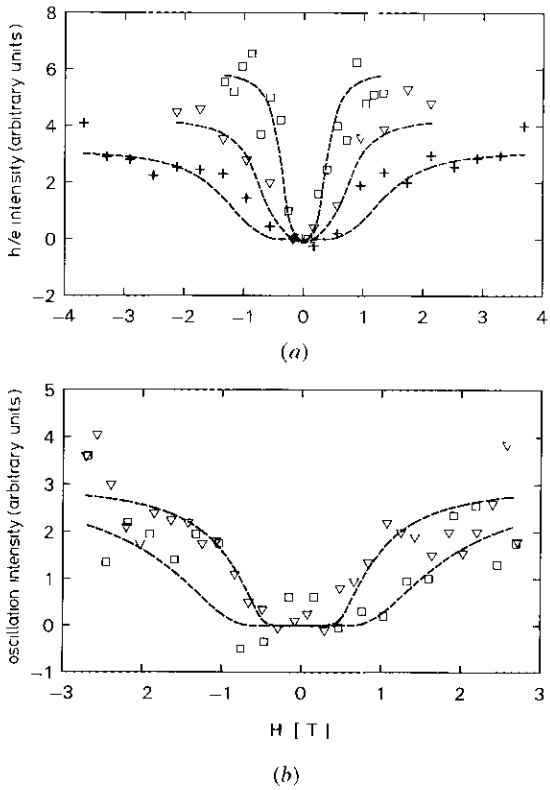

Figure 23 (a) The r m s amplitude of the h/e oscillations, in the presence of paramagnetic impurities, as a function of magnetic field at three temperatures $T = 0.06$ K (□), 0 12 K (▽), 0 21 K (+) (b) The amplitudes of the h/e (▽) and $h/2e$ (□) oscillations as function of magnetic field The dashed curves are fits to the data using the same fitted value of the magnetic impurity concentration The theoretical value of $\Delta G[h/e]$ for $\mu_B g H \gg k_B T$ has been adjusted to account for energy averaging

this hypothesis has borne out this estimate (to within the scatter in the data) Figure 23(*b*) contains the amplitudes of the two sets of oscillations as a function of field The h/e oscillations (○) are recovered at a lower characteristic field than the $h/2e$ oscillations (●) Using the same value, N_S, one can fit both curves by simply including the extra factor of 2 in the path length

Both of these studies were performed with the paramagnetic spins on the surface of the device--not in the bulk The behaviour of the system with the same concentration of bulk impurities is not known The probability to form Kondo singlets is presumably larger for localized spins in the bulk, since the contact integral between the carriers and the local moment is larger These Kondo singlets are not expected to destroy the oscillations completely at low fields since they carry no moment [97] The likelihood of spin-glass freezing of the localized spins may also be greater in the bulk Exchange with the random local moments [97] will be less damaging to the oscillation amplitude, since these moments are frozen, making exchange less likely

14. Experiments on semiconductor devices

Metal-oxide semiconductor field-effect transistors (MOSFETs) have proved to be useful devices in the study of conductance fluctuations, because semiconductors generally have higher diffusion coefficients and, therefore, larger E_c--frequently a few kelvin Assuming phase coherence can be maintained, this makes access to the $T=0$ K limit easier By changing the gate voltage, one can change the Fermi level This flexibility opens the avenue to a different class of experiments

An elegant observation of the correlated energy bands was made by tuning the gate voltage (and thereby the Fermi energy) of a MOSFET [115] In that experiment, the local fluctuation pattern was found to be invariant under small changes in E_F, and to change rather sharply once $\Delta E_F > E_C$, whereupon it remained fairly constant again until $\Delta E_F > 2E_C$ and another band was crossed Under the assumption that the Zeeman terms in G are irrelevant, this made a very nice demonstration of the existence of neighbouring bands of internally correlated levels

In another study [116], the plane of the sample was tilted relative to the magnetic field With **H** perpendicular to the plane of the device, a certain correlation field was observed When the device was tilted, the correlation field seemed to increase as expected for orbital motion confined to the plane of the MOSFET Similar experiments on GaAs samples [117, 118] have confirmed [117] that the correlation field scale grows as expected when the sample is tilted

One of the important realizations that has emerged from the theoretical work on universal conductance fluctuations is that they should persist into the regime of very large samples and high temperatures [118] This is simply the result of the weak algebraic averaging Several experiments on very narrow channel MOSFETs have been accomplished [119] which test the predictions about averaging of ΔG as a function of conductance, width and length of the device All of the experimental results are in support of the theory

We are ignoring in this discussion the research in the insulating regime (also called 'strong localization') where conductance fluctuations [120] as large as $\Delta g/g \gtrsim 10^2$ ($g \ll 1$) are commonly observed [121–125] In this case, the conduction processes are not coherent in the sense which we discuss in this paper—the carrier wavefunctions are not extended so they do not coherently span the device The electrons in strongly localized samples traverse the device by Mott hopping [126 128] among localized states or by resonantly tunnelling [129 130] through a particular localized state In the

case of Mott hopping, the conductance fluctuations can be an indirect count of the number of available hopping sites near the Fermi surface, and in the resonant tunnelling case, the fluctuation peaks are a more or less direct measures of the width and position of the individual energy level being sampled [131] and of the perturbations on that level caused by neighbouring sites [123, 132]

15. Magnetic field asymmetries: Onsager relations

Since the first data from the experiments, it has been apparent that the measured resistance is *not* a symmetric function of the magnetic field [75, 76, 133] This observation was a little unsettling at first, because there are strong arguments that the resistance should be absolutely symmetric about $H=0$ In large systems, the symmetry $G(H)=G(-H)$ is equivalent to (and results from) microscopic time-reversal symmetry [134, 135]

The observation has prompted several theoretical discussions which have attempted to resolve the origin of the asymmetry Upon looking more closely at the multichannel conductance formula (equation (6 1)), Buttiker and Imry [136] noticed that it was not symmetric about $\mathbf{H}=0$ For weak disorder ($l \simeq L$), the formula could have asymmetric components with relatively large amplitude The model invoked the experimental fact that the voltage measurements are made away from the reservoirs which supply and sink the current through the sample– that the measurements are done with four probes In contrast, the more widely accepted formula $g=\mathrm{Tr}\{\mathbf{t}\mathbf{t}^{\dagger}\}$, makes no such allowance and, hence, enforces the simple Onsager symmetry $G(H)=G(-H)$ The difficulty with this explanation is that in the experiments, $L \gtrsim 10\,l$ so that the conductance, according to conventional wisdom, should have conformed to $g=\mathrm{Tr}\{\mathbf{t}\mathbf{t}^{\dagger}\}$ and exhibited no asymmetry

Others have suggested that slight rearrangements of the spins on localized moments in the sample [97] can cause asymmetry in the conductance It was recently demonstrated that very small changes in the impurity configuration could completely rewrite the pattern of conductance fluctuations [97, 104] Based on this conclusion, Al'tshuler and Spivak [97] proposed that even very small changes in the orientations of local moments could account for the observed asymmetry It has also been noted that the quantum-mechanical analogue of the classical Hall voltage might fluctuate This prediction has been obtained both from linear response [63, 87, 137] and from direct calculation of the conductance using Landauer's approach [18, 100]

Very recently, Buttiker [73] has treated the four-probe geometry from the Landauer point of view and found that Onsager's symmetries are indeed conserved so long as they are defined for that measurement technique The voltage probes invariably measure some mixture of diagonal components R_{xx} and off-diagonal components of the resistance R_{xy} In general, these mixtures contain contributions from off-diagonal Onsager coefficients so that the symmetries are also mixed This gives rise to asymmetry in the measurement Moreover, the asymmetries which arise in this formulation require only phase coherence for the wavefunctions they do not require that $l \simeq L$ In fact, the quantum-mechanical conductance fluctuations mimic the symmetries found in classical electrodynamics [138–140]

The experiments [133] support the calculations of Buttiker [73] as far as symmetries in $G(H)$ are concerned Some of the experimental data are displayed in figure 24 The three traces correspond to three different arrangements of the leads The top trace $G_{14,23}$ is the result of current injected into 1 and withdrawn through 4 and a voltage drop measured from 2 to 3 The other two traces result from permutations of

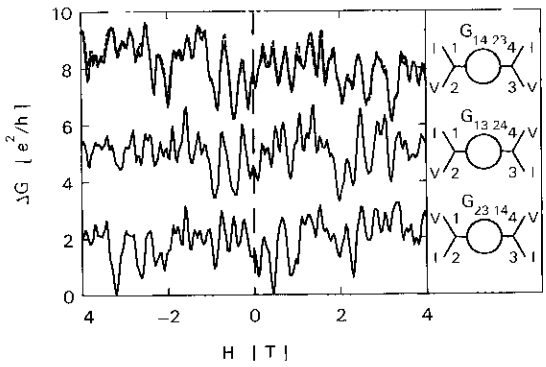

Figure 24 The variation of the conductance fluctuation pattern with different lead configurations The h/e oscillations have been filtered from the data for clarity of display The inset illustrates the measurement configuration for each of the traces

the voltage and current leads as illustrated in the inset The conductance measured for any particular arrangement of contact probes is related by some symmetry transformation to the conductance measured with the permuted leads If the current and voltage leads are interchanged, then the conductance is nearly mirror-symmetric through the plane $H=0$ This suggests that the measured conductance comprises a symmetric part and an antisymmetric part For a certain measurement configuration, the separation of these two parts is obtained from

$$G_S=2/[R_{14,23}(H)+R_{23,14}(-H)], \tag{15.1}$$

$$G_A=2/[R_{14,23}(H)-R_{23,14}(-H)] \tag{15.2}$$

When the conductance data are reduced according to these formulae, the resulting G_S and G_A (figure 25) are indeed nearly symmetric and antisymmetric, respectively The calculations of Buttiker predict just this set of symmetries for this measurement Short-range autocorrelation between $G_{14,23}$ and $G_{23,14}$ indicates that 90 per cent or more of the asymmetry results from G_A

The constructions can also be performed on individual measurements made with particular lead arrangements As demonstrated in figure 25 (b), all of the traces generate nearly the same G_S as is found from $2/[R_{14,23}(H)+R_{23,14}(-H)]$, and the r m s amplitude of all of the traces is $\Delta G_S=0.56\,e^2/h$ The symmetric part of G is not a function of the choice of current and voltage leads This result follows theoretically from the four-probe Landauer formula [73] in the restricted case of a very long (quasi-one-dimensional) sample

The data also support the predictions that the Hall voltage fluctuates The amplitude of the fluctuations in G_A build up over the course of a few fluctuations and then saturate at $\Delta G_A=0.44\,e^2/h$ The field scale associated with the antisymmetric fluctuations indicates that all of the phase coherent region of the wire (including the voltage probes) contributes to the fluctuations This field scale, however, is not independent of the shape of the sample [130], it just happens to be true for long samples All of these observations are consistent with the calculations by Ma and Lee [137]

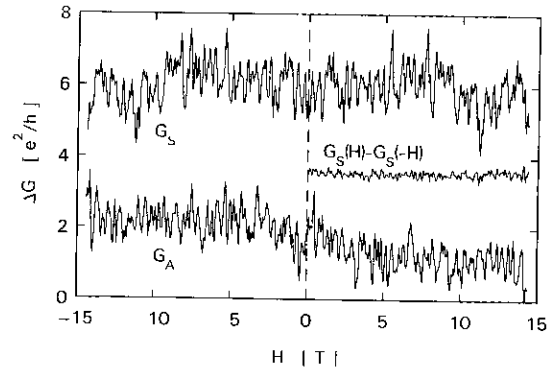

(*a*)

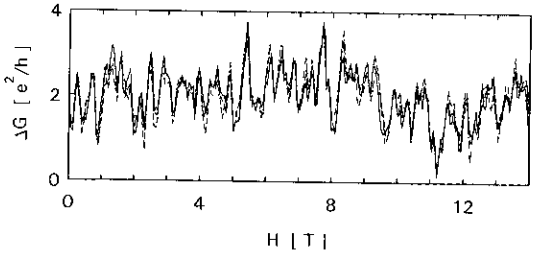

(*b*)

Figure 25 (*a*) The symmetric and antisymmetric components of the conductance constructed from $G_S = 1/R_S = 2/[R_{14\ 23}(H) + R_{23\ 14}(-H)]$, $G_A = 1/R_A = 2/[R_{14\ 23}(H) - R_{23\ 14}(-H)]$, and the residual asymmetry in $G_S = G_S(H) - G_S(-H)$ (*b*) The symmetric part of the conductance $G_S = 1/R_S = 2/[R_{ij\ mn}(H) + R_{ij\ mn}(-H)]$ for each of the traces in figure 24

A careful study (figure 26) of the Aharonov–Bohm oscillations near zero field has revealed that these too are not symmetric The oscillations have a random sample-dependent offset $0 < \beta < \pi$ from $H = 0$ Furthermore, the offset-β changes sign when the leads are permuted, as described above in the discussion of the random fluctuations (see figure 24) The origin of the offset (the parameter β in equation (6 3)) is certainly the asymmetry discussed by Buttiker [73] In contrast to the random fluctuations in G_A, this offset does not represent Hall voltages in the wires The finite value of β is an Aharonov-Bohm effect in the sense originally proposed for the free-electron case [4] — it is due to the gauge flux threaded through the loop

The finite values of β again confirm the phase coherence of the electron wavefunctions across the sample According to current understanding [73], the offset is the least robust of the interference manifestations In contrast to the aperiodic fluctuations, which suffer only algebraic averaging in the presence of inelastic scattering, the offset is finely dependent on coherence The presence of even slight phase-breaking in the device (particularly in the connecting leads) rapidly drives β to 0 or π

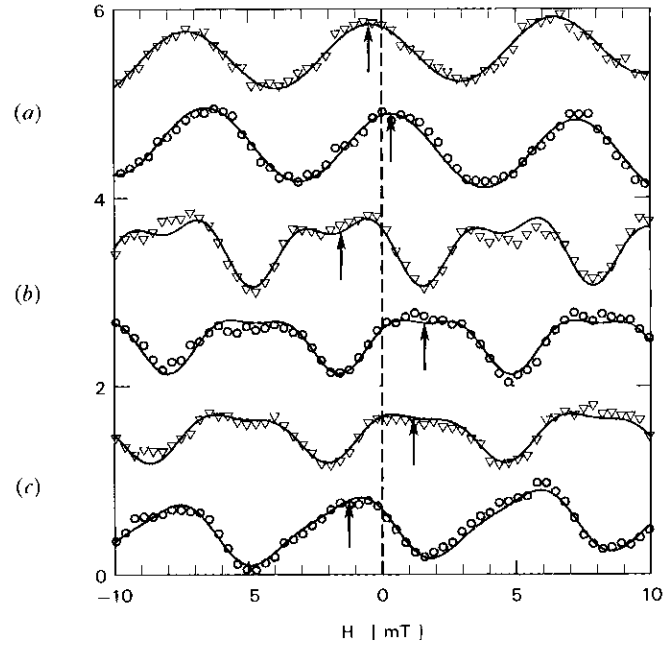

Figure 26 The Aharonov–Bohm oscillations at near-zero magnetic field illustrating the offset β which reverses sign when the leads are permuted The three pairs of traces are from three different samples having the same diameter (900 nm) The triangles and circles are $G_{14,23}$ and $G_{23,14}$, respectively The solid lines are fits to the data which account for a sloping background, an offset to the oscillations, and the amplitude of the oscillations In (*b*) and (*c*) account has also been taken of the $h/2e$ period present in the data The fitted offsets are (*a*) $-25°$ and $18°$, (*b*) $-86°$ and $89°$, and (*c*) $-63°$ and $66°$

16. Voltage fluctuations and universal conductance fluctuations: measurements with $L<L_\phi$

The results of the universal conductance theory were derived by calculating [51] the transmission coefficient for a long sample connected by two perfect leads to infinite reservoirs On the other hand, as pointed out in § 15, most of the experiments discussed here employ a four-probe measuring configuration The connecting leads are fabricated from the same material and must be included in the computation of the fluctuations Without losing phase coherence, electrons can propagate into the leads (in particular the voltage leads) up to a distance L_ϕ Recent experiments on lines and rings [141] have clearly proven that, when $L<L_\phi$, the measured voltage fluctuations are *independent* of the distance L between the voltage probes Upon converting this to conductance, one sees that the conductance fluctuations diverge as $(L_\phi/L)^2$ This is in direct contrast to the opposite limit $L>L_\phi$ where, as we have shown (equation (11 1)), $\Delta G \propto (L_\phi/L)^{3/2}$ Thus, when $L<L_\phi$, the conductance fluctuations are not universal in a four-wire measurement They are unbounded and can be very large This counter-intuitive result can be derived by considering what happens when four voltage leads are connected to a long line as shown in figure 27 (*a*) Considering the case where L_ϕ is greater than the largest separation between voltage probes and assuming that the voltages are additive (i e $V_{2,3}+V_{3,4}+V_{4,2}=0$) the measured voltage fluctuations between any two probes should depend only on the distance between voltage probes

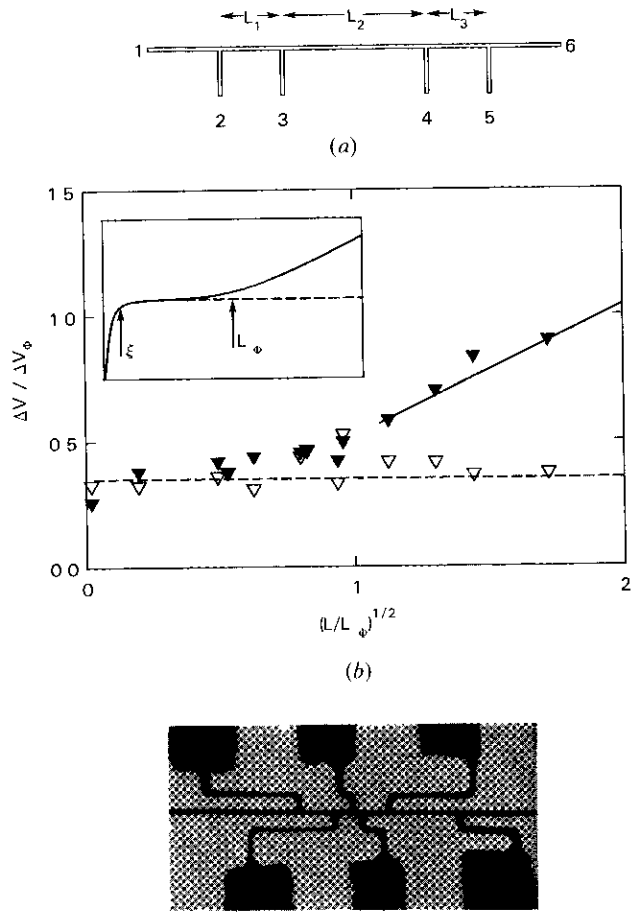

Figure 27 (*a*) Schematic for measurement of voltages along a wire as discussed in the text (*b*) The r m s amplitude of the antisymmetric part of the voltage fluctuations V_A (open symbols) and the symmetric part V_S solid symbols as a function of L_ϕ The inset shows schematically the expected behaviour of the voltage fluctuations as a function of length as discussed in the text (*c*) Electron microscope photograph of Sb sample

$\Delta V(L) \propto L^{\alpha}$ Using the general property that the voltage fluctuation of one term is less than or equal to the sum of the fluctuations of the other terms, one can write

$$\Delta V(L_1 + L_2) \leqslant \Delta V(L_1) + \Delta V(L_2), \tag{16 1}$$

$$\Delta V(I_1) \leqslant \Delta V(I_1 + L_2) + \Delta V(I_2) \tag{16 2}$$

By considering the two cases, $L_1 = L_2$ in equation (16 1) and $L_1 \to 0$ in equation (16 2), one can show $0 \leqslant \alpha \leqslant 1$ Using the symmetries discussed in §15 and forming the antisymmetric part of the voltage measures between leads 3 and 4, one can also show in general [141] that ΔV_A is a constant, independent of L The total fluctuation amplitude can never be smaller than the antisymmetric contribution, therefore a dependence

$\Delta V \propto L^{\alpha}$ with $\alpha > 0$ is not allowed for $L < L_\phi$. The final result is that the total measured voltage fluctuation is constant for $w < L < L_\phi$ (w is width of the wires). Similar considerations apply to the h/e periodic voltage oscillations measured between any two points on a ring [142].

As an example, the r.m.s. amplitude of the aperiodic voltage fluctuations measured in a long line is shown in figure 27 (*b*) as a function of L/L_ϕ. The data were obtained from Sb wires with voltage leads of similar dimension and material connected alternately to each side of the wire at varying distances. One of the samples used in these measurements is shown in figure 27 (*c*). By selecting different leads, fluctuations for 15 different lengths between 0.2 and 4 μm can be measured. As discussed in § 15, V_S and V_A were determined and are plotted as closed and open symbols, respectively. The data show that for all values of the sample length L, the antisymmetric part of the voltage fluctuations is constant, but the symmetric part of the voltage fluctuations is independent of length only for $L < L_\phi$. For lengths greater than L_ϕ the voltage fluctuations are increasing as $(L < L_\phi)^{1/2}$, in agreement with the discussion in § 11.

The point corresponding to $L \sim 0$ in figure 27 (*b*) was measured by injecting current into two adjacent leads and measuring the voltage between two leads 0.2 μm away from the classical current paths. However, the measured voltage fluctuations have the same value as those determined in a conventional resistance measurement so long as $L < L_\phi$. This measurement is proof that the fluctuations in voltage are in fact constant independent of the position of the voltage probes. It also demonstrates the importance of the propagation of the electrons into the leads. It is clear that the measured conductance fluctuations are not universal in a four-wire measurement and can be much larger than e^2/h. We emphasize that this is not inconsistent with the universal conductance fluctuation theory which only applies to a finite-length sample with two leads. In the case of $L \to 0$, however, the average voltage measured can be arbitrarily near zero. If we convert the average voltage to a resistance and use it to calculate conductance the r.m.s. voltage fluctuation for the point $L \sim 0$ in figure 27 (*b*) implies 'ΔG' $= 2 \times 10^6 e^2/h$. This shows that it is the voltage fluctuation and not the conductance fluctuation that should be considered when $L < L_\phi$. Experimentally, of course, the antisymmetric part of the fluctuations exists regardless of the geometrical arrangement of voltage probes. The explanation of the asymmetry in terms of a transverse voltage is not inconsistent with this result because the voltage fluctuations will not cancel for measurements on the same side, as it does for the classical Hall effect in a homogeneous rectangular bar [142]. The transverse voltage fluctuation can contain both symmetric and antisymmetric contributions. Experimentally only the symmetric part (longitudinal and transverse contribution) and the antisymmetric part (transverse only) can be determined.

Figure 28 (*a*) displays one of the most surprising experimental results obtained to date. The trace represents the non-local voltage fluctuations obtained from the measurement configuration shown in the inset. The measured average voltage $(V_1 - V_2)$ is nearly zero, while the r.m.s. fluctuation amplitude is the same as that measured along a segment of the line in the usual way $(V_3 - V_4)$ (so long as the distance between voltage probes are less than L_ϕ). Figure 28 (*b*) demonstrates a similar effect measured on a ring with six leads equally spaced around the perimeter. When current is applied to any two adjacent leads and voltage measured between leads on the opposite side of the ring, the amplitude of the h/e voltage oscillations are the same as from a measurement made using the standard configuration (see figure 9). Both these effects demonstrate the importance of voltage leads attached to the sample. Since the electron wavefunction

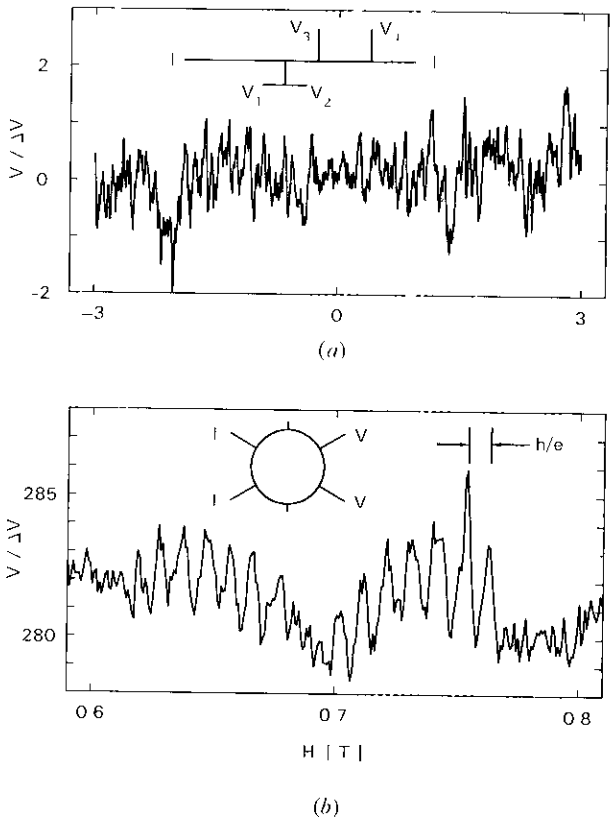

Figure 28 (*a*) Non-local voltage fluctuations $\Delta(V_1 - V_2)$ measured in a wire as illustrated in the inset (*b*) Non-local *h/e* oscillations in an Au loop with six leads measured as illustrated in the inset The non-local measurement and the conventional measurement (e g $V_3 - V_4$ in the inset (*a*)) yield the same fluctuation and oscillation amplitudes

exists everywhere within L_ϕ of a given point, voltage probes with $L < L_\phi$ will observe fluctuations having a field scale which is the same as that for probes which are separated by L_ϕ (The field scale will, of course, reflect the fact that the coherent region in the sample is no longer a simple rectangular slab)

A consequence of the power-law dependence of the voltage fluctuations $\Delta V(L) \propto L^\alpha$ is that the correlation function between different voltages measured on the same line depends on α The correlation C between measured voltages can be computed by noting that the voltages along the wire add For two adjoining segments of equal length, it can be shown that $C = \frac{1}{2}2^{2\alpha} - 1$ For $\alpha = 1$, there is complete correlation between voltages ($C = 1$), and for $\alpha = \frac{1}{2}$, there is no correlation between voltages ($C = 0$), and finally, for $\alpha = 0$, one finds $C = -\frac{1}{2}$ Figure 29 displays three voltage correlation functions, for the case of adjacent segments This figure illustrates the transition from a region without correlation ($L > L_\phi$, $\alpha = \frac{1}{2}$) to a region with negative correlation ($L < L_\phi$, $\alpha = 0$) The correlation measured for the smallest ratio ($L/L_\phi = 0\,25$) is $C = -0\,48 \pm 0\,07$ Of course, all correlations measured for non-adjacent segments are zero to within experimental error

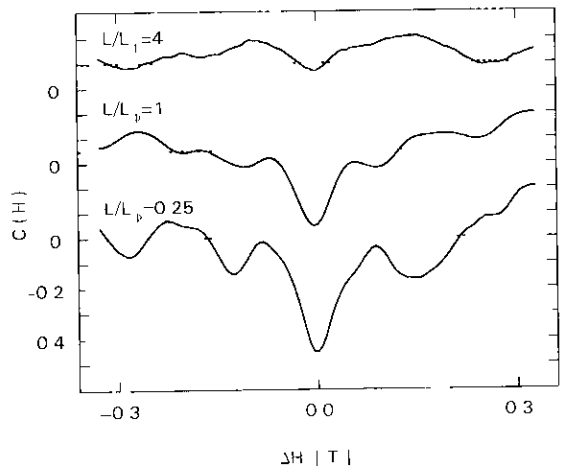

Figure 29 Cross-correlations between the voltages measured in adjacent line segments for the three different ratios L/L_ϕ

The length independence of the voltage fluctuations must break down when $L \to 0$. In the case of idealized one-dimensional probes, when $L=0$, ΔV must be zero. Therefore there must be a characteristic distance, below which the length independence breaks down and this is the subject of intensive theoretical and experimental investigation ([109, 144], Y Imry, P A Lee and S Maekawa and D Stone and W Skocpol, private communications). The current ideas [141] are that for lengths shorter than the mean free path in strictly one-dimensional samples, the voltage fluctuations must approach zero with decreasing length, $\alpha \leqslant 1$. For real samples and voltage probes with finite width and thickness, the result is still very much in question. The measured voltage fluctuations may also depend upon the cross-sectional area and the phase coherence length, as well as the mean free path.

17 Persistent currents and a.c. Josephson effects

In § 5 we mentioned that the energy of a closed normal metal loop is periodic in h/e and, in the absence of coupling to reservoirs cannot dissipate energy. Electrons encircling the loop behave just like electrons in an infinite periodic lattice with the unit cell equal to the circumference of the loop [145]. Calculating the band structure (see figure 5) for a one-dimensional loop one finds that, within a band, the energy of a single electron is a periodic function of flux threading the loop with period h/e. At a given value of Φ, the velocity of the carriers $dE/d\Phi$ alternates between adjacent bands. In general, for a constant flux applied to the ring, there will be a circulating current of a magnitude given by a sum over the velocities in all the occupied bands,

$$I(\phi) = -\frac{e}{L}\sum v_n(\phi), \tag{17.1}$$

where L is the circumference of the loop, and $v_n(\phi)$ is the velocity of the electrons in the nth band. The velocity $dE/d\Phi$ increases monotonically with n, and because of the near cancellation between pairs of filled bands, the current should be dominated by the last filled band. For very weak disorder, the bands should be similar to the free-electron case, but with increasing disorder (more elastic scattering) the bands become flatter and

the velocities smaller In addition, the presence of disorder will most likely produce local fluctuations within a given band so that $dE/d\Phi$ or the velocity could vary substantially within a band, and the near cancellation provided by adjacent bands might be less effective Quantitative theoretical techniques need to be applied to this problem in order to predict accurately the contribution of all the bands to the persistent current Assuming the probability for Zener tunnelling [56, 103, 146, 147] from one band to another is very small at $T \simeq 0$, this current cannot decay and can be considered as a real persistent current An upper estimate for the magnitude of this current can be obtained by using $I \sim ev_F/L$ For the ring in figure 9 (excluding the leads), ignoring the number of transverse channels for the moment, a persistent current of magnitude $I \sim 10^{-7}$ A is predicted The loop inductance is on the order of 10^{-12} H Assuming good coupling to a detector, a flux resolution of at least 10^{-21} Wb would be required to measure this signal This is close to the sensitivity of available d c SQUIDs

The arguments in § 5 give an estimate of the magnitude of the persistent current It would appear that the magnitude of the current should decrease with increasing transverse channel number, but quantitative estimates of the averaging law are lacking for the moment Similar reasoning, however, suggested the same reduction for the magnitude of the Aharonov–Bohm effect which is clearly not what has been observed The effects of finite temperature on the magnitude of the persistent current are not completely understood Theoretically, inelastic events cause the persistent current to fluctuate but do not suppress it [18, 56] In addition, the Zener tunnelling between the adjacent bands, might be a source of dissipation, but this is a controversial point [59, 146] From the discussion in § 10, the effect of finite temperature on the Aharonov–Bohm oscillations and aperiodic conductance fluctuations is not as severe as first expected Owing to a high degree of correlation between bands, the transport properties are not sensitive to temperature until $k_B T$ exceeds the typical correlation energy E_c In the case of persistent currents, it appears that when thermal energy comparable to the band-separation, transitions between bands become possible and are likely to lower the magnitude of the circulating current This suggests that for the ring of figure 9 temperatures less than 0 1 mK may be required to see the maximum persistent current This temperature could be 100 to 1000 times larger for semiconductors

If we were to apply a flux to the loop which increases linearly in time, the current in each band would oscillate periodically with a frequency $f = 2\pi eE/h$, where E is the induced electric field This is the Josephson frequency for a single electron If the flux varies slowly, and Zener tunnelling can be neglected, then the current is confined to the same bands The induced frequency must be kept small enough so that $\hbar\omega$ is less than the band separation, which means $f < 10^8$ Hz for the ring of figure 9 Experimental tests of these predictions promise to be very difficult, but they would serve to increase our understanding of dissipative processes and their time-scales in normal metals

18 Conclusions and speculation

Unanswered questions and partially answered questions remain The advances in understanding made in the past few years have, of course, opened new fields which have to be explored In this section, we list a few of the questions which might be successfully attacked with current technology

One of the conclusions of the conductance fluctuations theory is that a puzzle in the understanding of $1/f$ noise is now solved The noise which appears ubiquitously in

resistance measurements was mysterious, in that the switching of microscopic (single-particle) traps, which are the source of the noise, seemed to be a trivial perturbation on the resistance of the samples In short, the observed amplitude of the noise was far too great to be explained by such weak changes in the impurity potential The conductance fluctuation pattern is, however, *critically* dependent on the exact configuration of defects The movement of a *single* impurity causes fluctuations $\Delta g \sim 1$, i e it is as violent a change as moving all of the impurities No comparison was made between these calculations and the wealth of existing experimental data on $1/f$ noise [148], but along with weak averaging of the fluctuations, the critical dependence on impurity position appears to be a significant step toward explaining the amplitude of $1/f$ noise The experimental evidence, however, which bears on these predictions has wrought mixed conclusions at the time of this writing ([149 151], W Webb, private communication)

Two unsolved conundra have been mentioned already at the end of § 8, but there are more fundamental questions at hand The presence in the devices of Kondo interactions or the formation of spin-glass states [97] have not been investigated experimentally Experimental tests of the complete many-channel conductance formula (6 2) and the fluctuations near [152] the ballistic regime ($l \simeq L$) are among the topics which come to mind Other questions such as the description of the effect of superconductivity (and the proximity effect) on the fluctuations are being addressed at present It has also been noted that other transport coefficients, such as the thermoelectric effect [90, 98], can exhibit fluctuations

Excluding, of course, the h/e oscillations which had been predicted some time ago, many of the important conclusions about the fundamental physics of conduction mentioned in the previous sections were unknown before these experiments began The random fluctuations, and the theoretical work which they prompted, were completely unexpected In many ways, this aspect of the research has a further reach than the periodic effects The trend to study smaller devices at lower temperatures will focus on the case of coherent transport, and the predictions from the conductance fluctuation theory will bear on all of these investigations The speculations on the phase coherence of the electron wavefunctions in weakly disordered materials were clarified by the data from these studies Some hints had been obtained from the phase coherence of the time-reversed pairs which result in localization, but these were the first direct measurements of single phase-coherent electrons in disordered systems Even after due consideration we still find it rather miraculous that one can directly detect the interference of wavefunctions in a disordered system

Acknowledgments

We have benefited from many discussions with our colleagues, among them are A Benoit, M Buttiker, H Fukuyama, C van Haesendonck, Y Imry, R Laibowitz R Landauer, P Lee, M Ma, S Maekawa, F Milliken, D Stone and C Umbach

References

[1] Mermin, N D and Ashcroft, N W, 1976, *Solid State Physics* (New York Holt Rinehart and Winston)
[2] Landauer, R, 1957, *IBM J Res Dev*, **1**, 223
[3] Landauer, R, 1970, *Phil Mag*, **21**, 863
[4] Aharonov, Y, and Bohm, D, 1959, *Phys Rev*, **115**, 485
[5] Merzbacher, E, 1962, *Am J Phys*, **30**, 237
[6] Ehrenberg, W, and Siday, R E 1949, *Proc R Soc, Lond* B, **62**, 8
[7] Chambers R G 1960, *Phys Rev Lett*, **5**, 3

[8] MOLLENSTEDT, G, SCHMID, H, and LICHTI, H, 1982, *Proceedings of the Tenth International Congress on Electron Microscopy*, Hamburg (Deutschgesellschaft fur Elektronen Mikroskopie), p 434
[9] TONOMURA, A, MATSUDA, T, SUZUKI, R, FUKUHARA, A, OSAKABE, N, UMEZAKI, H, ENDO, J, SHINAGAWA, K SUGITA, Y, and FUJIWARA, H, 1982, *Phys Rev Lett*, **48**, 1443, 1986, Preprint
[10] DEAVER, B S JR, and FAIRBANK, W F, 1961, *Phys Rev Lett*, **7**, 43
[11] DOLL, R, and NABAUER, M, 1961, *Phys Rev Lett*, **7**, 51
[12] PARKS, R D, and LITTLE, W A, 1964, *Phys Rev* A, **133**, 97
[13] BRANDT, N B, GITSU, D V NIKOLAEVA, A A, and PONOMAREV, YA G, 1976, *JETP Lett*, **24**, 273, BRANDT, N B, BOGACHEK, E N, GITSU, D V, GOGADZE, G A, KULIK, I O, NIKOLAEVA, A A, and PONOMAREV, YA G, 1982, *Sov J low-temp Phys*, **8**, 358, GOGADZE, G A, 1983, *Sov J low-temp Phys*, **9**, 543
[14] KULIK, I O, 1967, *JETP Lett*, **5**, 345, 1970, *Ibid*, **11**, 275
[15] AL'TSHULER, B L, ARONOV A G, and SPIVAK, B Z, 1981, *JETP Lett*, **33**, 94
[16] LANDAUER, R, 1966, Internal memo, IBM Thomas J Watson Research Center
[17] GUNTHER, L, and IMRY, Y, 1969, *Solid St Commun*, **7**, 1391
[18] For a review see BUTTIKER, M, 1985, *SQUID-85 Superconducting Quantum Interference Devices and Their Applications*, edited by D-A Halbohm and H Lubbig (New York Walter-de Gruyter), p 529
[19] WEBB R A, WASHBURN, S, UMBACH C P, and LAIBOWITZ, R B, 1985, *Phys Rev Lett*, **54**, 2696
[20] CHANDRASEKHAR, V, ROOKS, M J, WIND, S, and PROBER, D E, 1985, *Phys Rev Lett*, **55**, 1610
[21] DATTA, S, MELLOCH, M R, BANDYOPADYAY, S, NORTN, R, VARIZI, M, MILLER, M, and REIFENBERGER, R, 1985, *Phys Rev Lett*, **55**, 2344
[22] DINGLE, R B, 1952, *Proc R Soc, Lond* A, **211**, 517
[23] DINGLE, R B, 1952, *Proc R Soc, Lond* A, **212**, 47
[24] LANDAUER, R, 1984, *Localization, Interaction, and Transport Phenomena in Impure Metals*, edited by G Bergmann Y Bruynseraede and B Kramer (Heidelberg Springer-Verlag) p 38
[25] BUTTIKER, M, 1986, *Phys Rev* A, **33**, 3020
[26] SHARVIN, D YU, and SHARVIN, YU V, 1981, *JETP Lett*, **34**, 272
[27] AL'TSHULER, B K, ARONOV, A G, SPIVAK, B Z, SHARVIN, D YU, and SHARVIN, YU V, 1982, *JETP Lett*, **35**, 588
[28] AL'TSHULER, B L, KHMEL'NITSKII D, LARKIN, A I, and LEE, P A, 1980, *Phys Rev* B, **22**, 5142
[29] LARKIN, A I and KHMEL'NITSKII, D E, 1982, *Sov Phys Usp*, **25**, 185
[30] GORKOV, L P, LARKIN, A I, and KHMEL'NITSKII, D E, 1979, *JETP Lett*, **30**, 228
[31] ABRAHAMS, E, ANDERSON, P W, LICIARDELLO D C, and RAMAKRISHNAN T V, 1979 *Phys Rev Lett*, **42**, 673
[32] LARKIN A I, 1980, *JETP Lett*, **31**, 219
[33] BISHOP, D J, DYNES R C, and TSUI, D C, 1982, *Phys Rev* B, **26**, 773
[34] BERGMANN, G, 1984, *Phys Rep*, **107**, 1
[35] CHAKRAVARTY, S, and SCHMID, A, 1986, *Phys Rep*, **140**, 193
[36] LEE, P A, and RAMAKRISHNAN, T V, 1985, *Rev mod Phys*, **57**, 287
[37] AL'TSHULER, B L and ARONOV, A G, 1985, *Electron–electron Interactions in Disordered Systems* edited by A L Efros and M Pollak (New York Elsevier), p 1
[38] FUKUYAMA, H, 1985, *Electron–electron Interactions in Disordered Systems*, edited by A L Efros and M Pollak (New York Elsevier), p 155
[39] SHABLO, A A, NARBUT, T P, TYURIN, S A, and DMITRENKO, I M, 1974, *JETP Lett*, **19**, 246
[40] SHARVIN, YU V, 1984, *Physica*, **126B**, 288
[41] LADAN, F R, and MAURER, J, 1983, *C r hebd Seanc Acad Sci, Paris*, **297**, 227
[42] GIJS, M, VAN HAESENDONCK, C, and BRUYNSERAEDE, Y, 1984, *Phys Rev Lett*, **52**, 2069, 1984, *Phys Rev* B, **30**, 2964
[43] GORDON, J M, 1984, *Phys Rev* B, **30**, 6770
[44] PANNETIER, B CHAUSSY, J, RAMMAL, R, and GANDIT, P, 1984, *Phys Rev Lett*, **53**, 718
[45] PANNETIER B, CHAUSSY, J, RAMMAL, R and GANDIT, P, 1984, *Phys Rev* B **31**, 3209

[46] Bishop, D J, Licini, J C, and Dolan, G J, 1985, *Appl Phys Lett*, **46,** 1000
[47] Dolan, G J, Licini, J C, and Bishop, D J, 1985, *Phys Rev Lett*, **56,** 1493
[48] Douçot B, and Rammal, R, 1985, *Phys Rev Lett*, **55,** 1148
[49] Stone, A D, 1985, *Phys Rev Lett*, **54,** 2692
[50] Al'tshuler, B L, 1985, *JETP Lett*, **41,** 648
[51] Lee P A, and Stone, A D, 1985, *Phys Rev Lett*, **55,** 1622
[52] Lee P A, Stone, A D, Fukuyama, H, 1986, *Phys Rev* B (to be published)
[53] Buttiker, M, Imry, Y, and Landauer, R, 1983, *Phys Lett*, **96A,** 365
[54] Byers, N, and Yang, C N, 1961, *Phys Rev Lett*, **7,** 46
[55] Bloch, F, 1970, *Phys Rev* B, **2,** 109
[56] Landauer, R, and Buttiker, M, 1985, *Phys Rev Lett*, **54,** 2049
[57] Buttiker, M, 1984, *Proceedings of the Conference Localization, Interaction, and Transport Phenomena in Impure Metals*, edited by G Bergmann, Y Bruynseraede and B Kramer (Heidelberg Springer-Verlag), p 107
[58] Buttiker, M, 1986 *Ann N Y Acad Sci*, **480,** 194
[59] Lenstra, D, and van Haeringen, W, 1986, *Phys Rev Lett*, **57,** 1623
[60] Lenstra, D and van Haeringen, W, 1985, *Physica*, **128B,** 26
[61] Fourcade, B, 1986 *Phys Rev* B, **33,** 6644
[62] Li Q, and Soukoulis, C M, 1986, *Phys Rev* B, **33,** 7318
[63] Vasilopoulis, P, and van Vliet, C M, 1985, Preprint
[64] Carini, J P, Muttalib, K A, and Nagel, S R, 1984, *Phys Rev Lett*, **53,** 102, Browne, D A, Carini, J P, Muttalib, K A and Nagel, S R, 1984, *Phys Rev* B, **30,** 6798, Browne, D A, Carini J P, and Nagel, S R, 1985, *Phys Rev Lett*, **55,** 136, Browne, D A, and Nagel, S R, 1985, *Phys Rev* B, **32,** 8424, Carini, J P, Browne, D A, and Nagel, S R, 1985, *Localization and Metal-Insulator Transitions*, edited by H Fritzsche and D Adler (New York Plenum), p 281
[65] Geffen, Y, Imry, Y, and Azbel, M Ya, 1984, *Surf Sci*, **142,** 203
[66] Geffen, Y, Imry, Y, and Azbel M Ya, 1984, *Phys Rev Lett*, **52,** 129
[67] Buttiker, M, Imry, Y, and Azbel, M Ya, 1984, *Phys Rev* A, **30,** 1982
[68] Murat, M, Giffen, Y, and Imry, Y, 1986, *Phys Rev* B, **34,** 659
[69] Buttiker, M, Imry Y, Landauer, R, and Pinhas, S, 1985, *Phys Rev* B, **31,** 6207
[70] Azbel M Ya, 1981, *J Phys* C, **14,** L225
[71] Engquist, H L and Anderson, P W, 1981, *Phys Rev* B **24,** 1151
[72] Anderson, P W, Thoulfss, D J, Abrahams, E, and Fisher D S, 1980, *Phys Rev* B, **22,** 3519
[73] Buttiker, M, 1986, *Phys Rev Lett*, **57,** 1761
[74] Broers, A N, 1973, *J vac Sci Technol*, **10,** 979, Laibowitz, B, and Broers, A N, 1982, *Treatise on Materials Science*, Vol 24, edited by K N Tu and R Rosenberg (New York Academic), p 285
[75] Webb, R A Washburn, S, Umbach, C P, and Laibowitz, R B, 1984, *Localization, Interaction, and Transport Phenomena in Impure Metals*, edited by G Bergmann, Y Bruynseraede and B Kramer (Heidelberg Springer-Verlag) p 121
[76] Umbach, C P, Washburn, S, Laibowitz, R B, and Webb, R A, 1984, *Phys Rev* B, **30,** 4048
[77] Hikami, S, Larkin, A I, and Nagaoka, Y, 1980, *Prog theor Phys*, **63,** 707
[78] Blonder, G, 1984, *Bull Am phys Soc*, **29,** 535
[79] Umbach, C P, 1984, *Bull Am phys Soc*, **29,** 535
[80] Lee, P A, and Fisher, D S, 1981, *Phys Rev Lett*, **47,** 882
[81] Gor'kov, L P, and Eliashberg, G M, 1965, *Sov Phys JETP*, **21,** 940
[82] Kubo, R, Kawabata, A, and Kobayashi, S, 1984, *Ann Rev mater Sci*, **14,** 49
[83] Webb, R A Washburn, S, Umbach, C P, and Laibowitz, R B, 1986 *J Magn magn Mater*, **54–57,** 1423
[84] Umbach, C P Washburn, S, Webb, R A, Koch, R, Bucci, M, Broers, A N, and Laibowitz R B, 1986, *J vac Sci Technol* B, **24,** 383
[85] Webb, R A, Washburn, S, Umbach, C P, and Laibowitz R B, 1985, *SQUID-85 Superconducting Quantum Interference Devices and Their Applications*, edited by D-A Halbohm and H Lubbig (New York Walter-de Gruyter) p 561
[86] Edwards S F 1958 *Phil Mag*, **3,** 10 ··

[87] AL'TSHULER, B L, and KHMEL'NITSKII, D E, 1985 *JETP Lett*, **42,** 359
[88] MALDAGUE, P F, 1981, *Phys Rev* B, **23,** 1719
[89] IMRY, Y, 1986, *Europhys Lett*, **1,** 249
[90] PICHARD, J L, and SARMA, G, 1981, *J Phys* C, **14,** L127, PICHARD, J L, and ANDRE, G, 1986, *Europhys Lett*, **2,** 477
[91] IMRY, Y, 1986, 'Physics of mesoscopic systems' in *Directions in Condensed Matter Physics*, edited by G Grinstein and E Mazenko (Singapore World Publishing), pp 101–163
[92] THOULESS, D J, 1977, *Phys Rev Lett*, **39,** 1167
[93] LEE, P A 1986 *Physica*, A, **140** (to be published)
[94] SIVAN, U, and IMRY, Y, 1986 (to be published)
[95] AL'TSHULER, B L, and SHKLOVSKII, B I, *Soviet Phys JETP* (submitted)
[96] AL'TSHULER, B L, KRAVTSOV, V E, and LERNER, I V, 1986, *JETP Lett*, **43,** 441
[97] AL'TSHULER, B L, and SPIVAK, B Z, 1985, *JETP Lett*, **42,** 447
[98] SIVAN, U, and IMRY, Y, 1985, *Phys Rev* B, **33,** 551
[99] IMRY, Y, and SHIREN, N, 1986, *Phys Rev* B, **33,** 7992
[100] ENTIN-WOHLMAN, O, HARTZSTEIN, K, and IMRY, Y, 1986, *Phys Rev* B, **34,** 921
[101] ARONOV, A G, ZYUZIN, A YU and SPIVAK, B Z, 1986, *JETP Lett*, **43,** 555
[102] SHAPIRO, B, 1986, *Phys Rev* B, **34,** 4394
[103] VASILOPOULOS, P, and VAN VLIET, C M, 1986, *Phys Rev* B, **34,** 4375
[104] FENG, S, LEE, P A, and STONE, A D, 1986, *Phys Rev Lett*, **56,** 1960
[105] SAK, J and KRAMER, B, 1981, *Phys Rev* B, **24,** 1761
[106] BUTTIKER, M, 1986, Quantum interference in small metallic rings in a magnetic field, Preprint
[107] KHMEL'NITSKII, D E, and LARKIN, A I, 1986, *Soviet Phys JETP* (to be published)
[108] STONE A D, and IMRY, Y, 1986, *Phys Rev Lett*, **56,** 189
[109] ISAWA, Y, EBISAWA, H, and MAEKAWA S, 1986, *J phys Soc Japan*, **55,** 2523
[110] WASHBURN, S, UMBACH, C P, LAIBOWITZ, R B, and WEBB, R A, 1985, *Phys Rev* B, **32,** 4789
[111] UMBACH, C P, VAN HAESENDONCK, C, LAIBOWITZ, R B, WASHBURN S, and WEBB, R A, 1986, *Phys Rev Lett*, **56,** 386
[112] WEBB, R A, WASHBURN, S, UMBACH, C P, MILLIKEN, F P, LAIBOWITZ, R B and BENOIT, A D, 1987, *Physica* A, **140** (to be published), and *Phys Rev* B (to be published)
[113] SANTHANAM, P, WIND, S, and PROBER, D E, 1984, *Phys Rev Lett*, **53,** 1179
[114] BENOIT, A D, WEBB, R A, WASHBURN, S, UMBACH, C P, and LAIBOWITZ, R B 1986 (to be published)
[115] LICINI, J C, BISHOP, D J, KASTNER, M A, and MELNGAILIS, J, 1985, *Phys Rev Lett*, **55,** 2987
[116] KAPLAN, S B, and HARTSTEIN, A, 1986, *Phys Rev Lett*, **56,** 2403
[117] WHITTINGTON, C P, MAIN, P C, EAVES, L, TAYLOR, R P, THOMS, S, BEAUMONT, S P, and WILKINSON, C D W, 1986, Universal conductance fluctuations in the magnetoresistance of submicron n^+ GaAs wires, Preprint
[118] ISHIBASHI, K, NAGATA, K, GAMO, K, NAMBA, S, ISHIDA, S, MURASE K, KAWABE, M, and AOYAGI, Y, 1986, *Jpn J phys Soc* (to be published)
[119] SKOCPOL, W J, MANKIEWICH, P M, HOWARD, R E, JACKEL, L D, TENNANT, D M, and STONE, A D, 1986, *Phys Rev Lett*, **56,** 2865
[120] HOWARD, W E, and FANG, F F, 1965, *Solid St Electron*, **8,** 82
[121] FOWLER, A B, HARTSTEIN, A, and WEBB, R A, 1982, *Phys Rev Lett*, **48,** 196
[122] WEBB, R A, HARTSTEIN, A, WAINER, J J, and FOWLER, A B, 1985, *Phys Rev Lett*, **54,** 1577
[123] FOWLER, A B, TIMP, G L, WAINER, J J, and WEBB, R A, 1986, *Phys Rev Lett*, **57,** 138
[124] KWASNIK, R F, KASTNER, M A, MELNGAILIS, J, and LEE, P A, 1984, *Phys Rev Lett*, **52,** 224
[125] DEAN, C C and PEPPER, M, 1982, *J Phys* C, **15,** L617
[126] LEE, P A, 1984, *Phys Rev Lett*, **53,** 2042
[127] NGUYEN, V L, SPIVAK, B Z, and SHKLOVSKII, B I, 1984, *JETP Lett*, **41,** 42 1985, *Sov Phys JETP*, **62,** 1021
[128] RAIKH, M É, and RUZIN, I M, 1986, *JETP Lett*, **43,** 562
[129] LIFSHITZ, L M, and KIRPICHENKOV, V YA, 1979, *Sov Phys JETP*, **50,** 499

[130] AZBEL, M YA, 1983, *Solid St Commun*, **45,** 527
[131] STONE, A D, and LEE, P A, 1985, *Phys Rev Lett*, **54,** 1196, STONE A D, AZBEL, M YA, and LEE, P A, 1985, *Phys Rev* B, **31,** 1707
[132] KALIA, R K XUE, W and LEE P A, 1986, *Phys Rev Lett*, **57,** 1615
[133] BENOIT, A D, WASHBURN, S WEBB, R A, UMBACH, C P, and LAIBOWITZ, R B 1986, *Phys Rev Lett* **57,** 1765
[134] KASIMIR H B G 1945 *Rev mod Phys* **17,** 343
[135] ONSAGER L, 1931 *Phys Rev*, **38,** 2265
[136] BUTTIKER, M and IMRY, Y 1985 *J Phys* C **18,** L467
[137] MA, M, and LEE, P A 1986, Transverse conductance fluctuations and magnetic field asymmetry, Preprint
[138] VAN DER PAUW, L J 1958, *Philips Res Rep*, **13,** 1
[139] LANDAU, L D, and LIFSHITZ, E M, 1960, *Electrodynamics of Continuous Media* (New York Pergamon) p 92 et seq
[140] SAMPLE, H H, BRUNO, W J, SAMPLE, S B, and SICHEL, E K, 1987, *Phys Rev* B (submitted)
[141] BENOIT, A D, UMBACH, C P, LAIBOWITZ R B, and WEBB, R A, 1986, Preprint
[142] BENOIT, A D, WASHBURN, S, UMBACH, C P, LAIBOWITZ, R B and WEBB, R A, 1987, Effects of magnetic scattering on Aharonov Bohm oscillations in normal metal (in preparation)
[143] BRUIS, G J C L, BASS J, VAN GELDER, A P, VAN KEMPEN, H, and WYDER, P, 1981, *Phys Rev Lett*, **46,** 553
[144] BUTTIKER, M, 1986, Voltage fluctuations in small conductors, Preprint
[145] SVIRSKII, M S, 1985, *JETP Lett*, **42,** 270
[146] LANDAUER, R, 1986, *Phys Rev* B, **33,** 6497
[147] GEFEN, Y, BEN-JACOB, E, and CALDEIRA A O, 1986, Zener transitions in dissipative driven systems, Preprint
[148] Recent reviews can be found in DUTTA, P, and HORN, P M, 1981 *Rev mod Phys*, **53,** 497 KOGAN, SH M, 1985, *Sov Phys Usp*, **28,** 170
[149] RAILS, K S, SKOCPOL, W J JACKEL, L D, HOWARD R E FETTER, L A EPWORTH, R W, and TENNANT, D M, 1984, *Phys Rev Lett*, **52,** 228
[150] ROGERS, C T, and BURHMAN, R A, 1985, *Phys Rev Lett*, **55,** 859
[151] KOCH, R, FENG, S, LAIBOWITZ, R B, LACEY, J A and VIGGIANO, J M, 1986 Preprint
[152] TESANOVIC, Z JARIC, M V, and MAEKAWA, S, 1986, *Phys Rev Lett*, **57,** 2760